Summer 8-11-2015

Numerical Solutions of Generalized Burgers' Equations for Some Incompressible Non-Newtonian Fluids

Yupeng Shu
The University of New Orleans, yshu@uno.edu

Numerical Solutions of Generalized Burgers' Equations for Some Incompressible Non-Newtonian Fluids

A Thesis

Submitted to the Graduate Faculty of the
University of New Orleans
in partial fulfillment of the
requirements for the degree of

Master of Science
in
Mathematics

by

Yupeng Shu

University of New Orleans, 2015
August 2015

Acknowledgements

I would like to give my sincere thanks to **Professor Dongming Wei**, who spent a lot of time on my study since I started research in mathematics. Professor Wei also examined the research of this thesis with great carefulness and guided me to make progress step by step, without which, I firmly believe that, there is still a long journey to the completion of this thesis. As an excellent scientific researcher, Professor Wei taught me a lot of research methods in applied mathematics; as a trust-worthy elder, he gave me advice in academia and life as well.

I would also like to give my sincere thanks to the other two committee members,

Professor Jairo Santanilla Department of Mathematics, College of Science, the University of New Orleans

Professor Kenneth Holladay Department of Mathematics, College of Science, the University of New Orleans

their suggestions gave me ideas on how to optimize this manuscript. I want to give my sincere thanks to **Professor Juliette Ioup** from the Department of Physics and **Professor Ralph Saxton** from the Department of Mathematics for their help in proof-reading this manuscript. In addition, I acknowledge the great support from the faculty and staff of the College of Science and the College of Engineering on my routine study and coursework. I acknowledge the support from the faculty and staff of College of Liberal Arts on my study of the English language and American culture. I also acknowledge the great help on my daily life from administrators at student housing, graduate school, academic affairs, and student affairs at the University of New Orleans.

I would like to give my sincere thanks to my elementary school teachers, my middle school teachers, and my senior high school teachers in China for my education before I came to the United States of America for undergraduate study. I will never forget those people who helped me after I came to the United States of America. Finally, I especially would like to give my sincere gratitude to my parents, my grandparents, and my other relatives for their continuing support on me.

Yupeng Shu

Department of Mathematics
University of New Orleans
New Orleans LA 70148
The United States of America
August, 2015

Contents

Acknowledgements iii

Contents v

List of Figures viii

List of Tables ix

Symbols x

Abbreviations xi

Abstract xii

1 Introduction 2
1.1 Newtonian and Non-Newtonian Viscous Fluids 2
1.2 The Navier-Stokes Equations 2
1.3 The Constitutive Equation 3
1.4 Equation of Flow on the x-axis 4
1.5 Outline of the Thesis 4

2 Derivation of Generalized Burgers' Equation for Some Non-Newtonian Fluids 6
2.1 Incompressible and Isothermal Viscous Fluids 6
2.2 Three Rheology Models 7

3 Traveling Wave Solutions of Burgers' Equation based on the Cross Model 8
3.1 Derivations of Burgers' Equations for the Cross Model 8
3.2 Fluid 1 of the Cross Model 9
3.2.1 Plots for Fluid 1 of the Cross Model with the Integral Term 11
3.2.2 Plots for Fluid 1 of the Cross Model without the Integral Term . . 12

4 Traveling Wave Solutions of Burgers' Equation based on the Carreau Model 15
4.1 Burgers' Equation for the Carreau Model 15

4.2 Fluid A of the Carreau Model . . . 15
4.2.1 Plots for Fluid A of the Carreau Model with the Integral Term . . 16
4.2.2 Plots for Fluid A of the Carreau Model without the Integral Term 17

5 Traveling Wave Solutions of Burgers' Equation based on the Power-Law Model 20
5.1 Burgers' Equation for the Power-Law Model . . . 20
5.2 Fluid Mayonnaise of the Power-Law Model . . . 20
5.2.1 Plots for Fluid 1 of the Power-Law Model with the Integral Term . 21
5.2.2 Plots for Fluid 1 of the Power-Law Model without the Integral Term 22

6 Existence and Uniqueness of Solutions to the Traveling Wave Equations 25
6.1 Existence and Uniqueness of Solutions . . . 25
6.2 Existence and Uniqueness of Solutions for the Cross Model with the Integral Term . . . 26
6.2.1 Continuity of $\frac{\partial F}{\partial u'}$ . . . 26
6.2.2 Continuity of $\frac{\partial F}{\partial u}$ . . . 27
6.3 Existence and Uniqueness of Solutions for the Cross Model without the Integral Term . . . 27
6.3.1 Continuity of $\frac{\partial F}{\partial u'}$ . . . 27
6.3.2 Continuity of $\frac{\partial F}{\partial u}$ . . . 28
6.4 Existence and Uniqueness of Solutions for the Carreau Model with the Integral Term . . . 28
6.4.1 Continuity of $\frac{\partial F}{\partial u'}$ . . . 29
6.4.2 Continuity of $\frac{\partial F}{\partial u}$ . . . 29
6.5 Existence and Uniqueness of Solutions for the Carreau Model without the Integral Term . . . 30
6.5.1 Continuity of $\frac{\partial F}{\partial u'}$ . . . 30
6.5.2 Continuity of $\frac{\partial F}{\partial u}$ . . . 30
6.6 Existence and Uniqueness of Solutions for the Power-Law Model with the Integral Term . . . 31
6.6.1 Continuity of $\frac{\partial F}{\partial u'}$ . . . 31
6.6.2 Continuity of $\frac{\partial F}{\partial u}$ . . . 32
6.7 Existence and Uniqueness of Solutions for the Power-Law Model without the Integral Term . . . 32
6.7.1 Continuity of $\frac{\partial F}{\partial u'}$ . . . 32
6.7.2 Continuity of $\frac{\partial F}{\partial u}$ . . . 33
6.8 Theorem on Existence and Uniqueness of Solutions for all Three Models . 33

7 The Order of Thickness of the Transition Layers 34
7.1 Derivations and Formulas . . . 34
7.2 Tables and Discussion . . . 34

8 Conclusion 36

A MATLAB Codes **37**

A.1 MATLAB Codes for fluid 1 of the Cross Model with the Integral Term . . 37

A.2 MATLAB Codes for Fluid 1 of the Cross Model without the Integral Term 40

A.3 MATLAB Codes for Fluid 1 of the Carreau Model with the Integral Term 41

A.4 MATLAB Codes for Fluid A of the Carreau Model without the Integral Term 43

A.5 MATLAB Codes for Fluid Mayonnaise of the Power-Law Model with the Integral Term 45

A.6 MATLAB Codes for Fluid Mayonnaise of the Power-Law Model without the Integral Term 48

B MATLAB Information **51**

Bibliography **52**

Vita **55**

List of Figures

3.1 Wave Profile $u(x)$ for the Cross Model with the Integral Term 11
3.2 $u'(x)$ for the Cross Model with the Integral Term 12
3.3 Velocity Vectors for the Cross Model with the Integral Term 12
3.4 Wave Profile $u(x)$ for the Cross Model without the Integral Term 13
3.5 $u'(x)$ for the Cross Model without the Integral Term 13
3.6 Velocity Vectors for the Cross Model without the Integral Term 14

4.1 Wave Profile $u(x)$ for the Carreau Model with the Integral Term 16
4.2 $u'(x)$ for the Carreau Model with the Integral Term 17
4.3 Velocity Vectors for the Carreau Model with the Integral Term 17
4.4 Wave Profile $u(x)$ for the Carreau Model without the Integral Term . . . 18
4.5 $u'(x)$ for the Carreau Model without the Integral Term 18
4.6 Velocity Vectors for the Carreau Model without the Integral Term 19

5.1 Wave Profile $u(x)$ for the Power-Law Model with the Integral Term 21
5.2 $u'(x)$ for the Power-Law Model with the Integral Term 22
5.3 Velocity Vectors for the Power-Law Model with the Integral Term 22
5.4 Wave Profile $u(x)$ for the Power-Law Model without the Integral Term . . 23
5.5 $u'(x)$ for the Power-Law Model without the Integral Term 23
5.6 Velocity Vectors for the Power-Law Model without the Integral Term . . . 24

List of Tables

7.1 Shock Thickness and Maximum Strain ε_{11} for Fluid 1 of the Cross Model 35
7.2 Shock Thickness and Maximum Strain ε_{11} for the Fluid A of the Carreau Model 35
7.3 Shock Thickness and Maximum Strain ε_{11} for the Fluid Mayonnaise of the Power-Law Model 35

Symbols

p_x	horizontal component of pressure gradient	Pa/m
p_y	vertical component of pressure gradient	Pa/m
p	pressure	Pa
u	horizontal component of fluid velocity	m/s
v	vertical component of fluid velocity	m/s
$\vec{f}$	external force	N/m
x	position in the horizontal direction	m
y	position in the vertical direction	m
n	power-law exponent for all models	
ρ	fluid density	kg/m^3
$\vec{\nu}$	fluid velocity	m/s
τ_{ij}	element in stress tensor where $i, j = 1, 2$	N/m
ε_{ij}	element in strain tensor where $i, j = 1, 2$	$1/s$
η	apparent viscosity	$Pa\ s$
γ	shear rate	$1/s$
α	parameter in the Carreau-Yasuda model	
η_o	asymptotic value of η for zero shear rate	$kg\ m^{-1}s^{-1}$
η_∞	asymptotic value of η for infinite shear rate	$kg\ m^{-1}s^{-1}$
κ	time constant from referenced resource	s
$\bar{\kappa}$	time constant	s

Abbreviations

ODE **O**rdinary **D**ifferential **E**quation

PDE **P**artial **D**ifferential **E**quation

Abstract

We present some generalized Burgers' equations for incompressible and isothermal flow of viscous non-Newtonian fluids based on the Cross model, the Carreau model, and the Power-Law model and some simple assumptions on the flows. We numerically solve the traveling wave equations for the Cross model, the Carreau model, the Power-Law model by using industrial data. We prove existence and uniqueness of solutions to the traveling wave equations of each of the three models. We also provide numerical estimates of the shock thickness as well as maximum strain ε_{11} for each of the fluids.

Key words: Numerical solutions;
Generalized Burgers' equation;
Non-Newtonian fluid flows;
First-order implicit ODE;
Existence and Uniqueness of Solutions.

AMS 2010 Subject Classification: 34K28, 35C07, 76A05, 76A10, 76D03, 76D99

Dedicated to the people who love mathematics, science, and engineering.

Chapter 1

Introduction

1.1 Newtonian and Non-Newtonian Viscous Fluids

A Newtonian viscous fluid has a linear relation between the shear stress and the strain rate [37]. A non-Newtonian fluid has a nonlinear wave profile [22]. The viscosity of a non-Newtonian fluid varies with a different shear rate in the fluid, the container of the fluid, or even the initial condition of the fluid [22].
Newtonian fluids are ideal cases that are author seldom met in real life [37]. In reality, most fluids that people study are non-Newtonian fluids like blood, paints, wet mud and clay, and the majority of colloids [37]. Many non-Newtonian fluids can be modeled with the following three rheological models: the Cross, the Carreau, and the Power-Law models.The Cross and Carreau models cover the entire shear rate range[2],[22], and they can be used for food and beverages [2],[16] and blood flow [2],[29].The Power-Law model is applicable to many polymers and food fluids[2],[16].
In this thesis, we use industrial data for each type of fluids for numerical simulations.

1.2 The Navier-Stokes Equations

It is well known that the Navier-Stokes equation for viscous planar flows is based on the following equations[4],[5],[6],[11]

$$\begin{cases} \rho\left(u_t + uu_x + vu_y\right) = \tau_{11,x} + \tau_{12,y} - p_x + f_1 \\ \rho\left(v_t + uv_x + vv_y\right) = \tau_{21,x} + \tau_{22,y} - p_y + f_2 \\ u_x + v_y = 0 \end{cases} \tag{1.1}$$

where $\vec{v} = (u, v)$ is the fluid velocity, ρ is the density, $\tau \triangleq \begin{pmatrix} \tau_{11} & \tau_{12} \\ \tau_{11} & \tau_{22} \end{pmatrix}$ is the stress tensor, $\nabla p = (p_x, p_y)$ is the pressure gradient, and $\vec{f} = (f_1, f_2)$ is the external force.

The strain tensor is $\varepsilon \triangleq \begin{pmatrix} \varepsilon_{11} & \varepsilon_{12} \\ \varepsilon_{21} & \varepsilon_{22} \end{pmatrix}$, where $\varepsilon_{11} = u_x$, $\varepsilon_{12} = \frac{1}{2}(u_y + v_x) = \varepsilon_{21}$, and $\varepsilon_{22} = v_y$. For viscous Newtonian fluids, $\tau = 2\mu\varepsilon$. For symmetric flow about the x-axis, the author assumes that $u(x, y, t) = u(x, t)$, then $u_y = 0$, $u_x + v_y = 0$ implies that $v = -yu_x+$ constant, $\varepsilon_{11} = u_x$, $\varepsilon_{21} = \varepsilon_{12} = \frac{1}{2}(u_y + v_x) = \frac{1}{2}v_x = -\frac{1}{2}yu_{xx}$, and $\varepsilon_{22} = v_y = -u_x$.

1.3 The Constitutive Equation

In general, the constitutive rheology equation for viscous fluids is given in the following form

$$\tilde{\sigma} = 2\eta(\dot{\gamma})\tilde{\varepsilon} \tag{1.2}$$

where $\tilde{\sigma}$ is the stress tensor; $\tilde{\varepsilon}$ is the strain tensor; and the function $\eta(\dot{\gamma})$, called the apparent viscosity, is determined experimentally for a variety of important fluids such as polymer fluids, drilling muds, melted metals, bio-fluids and liquid foods. For planar flows, the relationship between stress and strain tensors is given in the following form

$$\tilde{\sigma} \triangleq \begin{pmatrix} \tau_{11} & \tau_{12} \\ \tau_{21} & \tau_{22} \end{pmatrix} = 2\eta(\dot{\gamma}) \begin{pmatrix} \varepsilon_{11} & \varepsilon_{12} \\ \varepsilon_{21} & \varepsilon_{22} \end{pmatrix} \tag{1.3}$$

where η is a function of the shear rate $\dot{\gamma}$, $\dot{\gamma} = [2u_x^2 + 2v_y^2 + \frac{1}{2}(u_y + v_x)^2]^{\frac{1}{2}}$. If $2\eta = \mu$ =constant[13], equation (1.1) then reduces to

$$\begin{cases} \rho\left(u_t + uu_x\right) = \mu u_{xx} - p_x + f_1 \\ \rho\left(v_t + uv_x + vv_y\right) = -2\mu y u_{xxx} - p_y + f_2 \end{cases} \tag{1.4}$$

In the special case that $\nu = \frac{\mu}{\rho}$ and the term $\left(-\frac{p_x(x,0)}{\rho} + \frac{f_1(x,0)}{\rho}\right)$ is negligible (as it is close to zero), the first expression in equation (1.4) is reduced to

$$u_t + uu_x = \nu u_{xx} \tag{1.5}$$

which is the well-known Burgers' equation for viscous Newtonian fluids[6],[32] that we regard as the basic assumption in this thesis. It plays a fundamental role in understanding nonlinear convective behavior of fluids with dissipative viscous behavior.

The inviscid counterpart of equation (1.5) is

$$u_t + uu_x = -\frac{p_2}{\rho} + \frac{f}{\rho} \tag{1.6}$$

Equations (1.5) and (1.6) have been studied extensively as a mathematical model to explain and understand more complicated physical systems like traffic flows, gas dynamics, and shallow water waves, see, e.g., [8], [9], [12], [14], [15], [18], [19], [20], [21], [23], and [25] for details.

1.4 Equation of Flow on the x-axis

With the same assumption $u(x, y, t) = u(x, t)$ adopted in deriving (1.3), then
$\varepsilon_{11} = u_x, \varepsilon_{21} = \varepsilon_{12} = -\frac{1}{2}yu_{xx}, v_x = -yu_{xx}$.
Substituting these expressions into (1.3), (1.1), and letting $y = 0$ in the result, then

$$\rho(u_t + uu_x) = 2(\eta(\dot{\gamma})u_x)_x - \eta(\dot{\gamma})u_{xx} - p_x + f_1 \tag{1.7}$$

where $|\dot{\gamma}| = 2|u_x|$ at $y = 0$.
For the Power-Law fluids, $\eta(\dot{\gamma}) = \mu|\dot{\gamma}|^{n-1}$, we have

$$\rho(u_t + uu_x) = \hat{\mu}(|u_x|^{n-1}u_x)_x - p_x + f_1 \tag{1.8}$$

where $u = u(x, 0, t), \hat{\mu} = \mu 2^{(n-1)}(\frac{2n-1}{n}), p_x = p_x(x, 0), f_1 = f_1(x, 0)$.
The analytic and numerical traveling wave solutions of an equation similar to (1.8) with the term $\left(-\frac{p_x(x,0)}{\rho} + \frac{f_1(x,0)}{\rho}\right)$ are provided in [5], [6]. Some nonlinear Burgers-type equations similar to equation (1.8) were studied extensively as a mathematical model in [1], [3], [17], [32], and [36], where the operator on the right hand side is $\nu(\frac{u_x}{1+u_x^2})_x$ and ν is a constant.

1.5 Outline of the Thesis

In this thesis, we study the Burgers' equations of this type derived from the following three rheological non-Newtonian fluids: the Cross, the Carreau, and the Power Law flows, and numerically calculates the corresponding traveling wave solutions to these equations. These three rheology models are widely adopted in chemical engineering, food processing, and petro-chemical engineering communities , see [16], [23], [24], [26], [27], [28], [35], and [37] for derivations and applications.
In the following sections, we denote $\tau_{11}(x, 0, t)$ by σ and $\varepsilon_{11}(x, 0, t) = u_x(x, 0, t)$ by u_x.

The assumption $u(x, y, t) = u(x, t)$ is not realistic in engineering applications and the resulting Burgers' equations provide only a partial flow velocity solution $u = u(x, 0, t)$, i.e., the flow velocity distribution on the x-axis as shown by the velocity plots in Chapters 3, 4, and 5. For simplicity, we also assume that $u(-L, 0, t) = 1$ and $u(L, 0, t) = 0$, where $L \leq \infty$. Understanding the solutions with these simple assumptions can provide insight into the more complicated flow patterns for these important fluids. Our numerical solutions and analysis indicate that the traveling wave solutions for these nonlinear Burgers' equations are all kink waves with various order of thickness of transition layers. For illustration and comparison purposes, we have chosen experimental data from science and engineering literature for certain industrial fluids as input parameters in the models for numerical evaluations. The resulting ordinary differential equations (ODEs) in $u(\xi), \xi = x - ct$ from these (PDEs) for traveling waves are all first order implicit equations, and therefore the MATLAB built-in ode15i() function is used for the numerical solutions. The use of the ode15i() function requires the value of $u_\xi(0)$ which are solved numerically by MATLAB's built-in fzero function before the numerical traveling wave solutions are calculated. The MATLAB codes are provided in the Appendix A. The details of information about the MATLAB platform that we use for computations are in Appendix B. Omitting the calculations used to obtain equation (1.8), we simply start with the Burgers' equations for each rheology model in the following sections. One of the purposes of this thesis is to show that there are several Burgers-type equations arising from studying non-Newtonian fluids which are similar to the one defined by the operator $\nu(\frac{u_x}{1+u_x^2})_x$ that intrigues mathematicians. In Chapter 2, we derive a general Burgers' equation for three non-Newtonian fluids. In Chapters 3, 4, and 5, we solve the traveling wave equation to the Burgers' equation with and without the integral term in equation (3.2), by using an implicit ODE solver named as MATLAB's built-in ode15i() function the fluids in the Cross model, the Carreau model, and the Power-Law model respectively. In Chapter 6, we implement the Peano theorem to prove the existence and uniqueness of solutions to the 1st-order ODE of the Cross model, the Carreau model, and the Power-Law model with and without the integral term in equation (3.2). In Chapter 7, we compute the thickness of transition layers and maximum strain ε_{11} for three models and compares the differences between the fluids with and without the integral term in equation (3.2).

Chapter 2

Derivation of Generalized Burgers' Equation for Some Non-Newtonian Fluids

2.1 Incompressible and Isothermal Viscous Fluids

Here we only consider incompressible, isothermal viscous fluids that satisfy equations (1.1) and (1.2). In addition, we assume that $u(x,y,t) = u(x,t)$, $v(x,0,t) = 0$, and $-p_x + f_1 = 0$. Because of these assumptions and the incompressibility equation $u_x + v_y = 0$, we have $u_y = 0$, $v = -yu_x, v_x = -yu_{xx}$, $\varepsilon_{21} = \varepsilon_{12} = \frac{1}{2}(u_y + v_x) = \frac{1}{2}v_x = -\frac{1}{2}yu_{xx}$, and $\varepsilon_{22} = v_y = -u_x$. Therefore the shear rate (1.2) is simplified to

$$\dot{\gamma} = \left\{ 2\left[u_x^2 + (-u_x)^2 + 2\left(-\frac{1}{2}yu_{xx}\right)^2 \right] \right\}^{\frac{1}{2}} = \left(4u_x^2 + y^2u_{xx}^2\right)^2 \tag{2.1}$$

Substituting equation (2.1) into the first equation of (1.1)and applying $u_y = 0$, we get

$$\rho\left(u_t + uu_x\right) = \left[2\eta\left(\dot{\gamma}\right)u_x\right]_x - \left[\eta\left(\dot{\gamma}\right)yu_{xx}\right]_y - p_x + f_1 \tag{2.2}$$

The right hand side of (2.2) can be rewritten as

$$2\eta(\dot{\gamma})_x u_x + \eta(\dot{\gamma})u_{xx} - \eta(\dot{\gamma})_y y u_{xx} \tag{2.3}$$

Since

$$\begin{cases} \eta(\dot{\gamma})_x = \eta'(\dot{\gamma})\dot{\gamma}_x = \frac{\eta'(\dot{\gamma})}{2\dot{\gamma}}(8u_x u_{xx} + 2y^2 u_{xx} u_{xxx}) \\ \eta(\dot{\gamma})_y = \eta'(\dot{\gamma})\dot{\gamma}_y = \frac{\eta'(\dot{\gamma})}{\dot{\gamma}} y u_{xx}^2 \end{cases} \tag{2.4}$$

Equation (2.2) becomes

$$\rho\left(u_t + uu_x\right) = \frac{\eta'(\dot{\gamma})}{\dot{\gamma}}(8u_x u_{xx} + y^2 u_{xx} u_{xxx})u_x + \eta(\dot{\gamma})u_{xx} - \frac{\eta'(\dot{\gamma})}{\dot{\gamma}} y^2 u_{xx}^3 \tag{2.5}$$

Letting $y = 0$, then from (2.2), we have

$$\rho\left(u_t + uu_x\right) = \left[2\eta\left(\dot{\gamma}\right)u_x\right]_x - \eta\left(\dot{\gamma}\right)u_{xx} - p_x\left(x,0\right) + f_1\left(x,0\right) \tag{2.6}$$

In particular, $\dot{\gamma} = 2|u_x|$, and we have

$$\rho\left(u_t + uu_x\right) = \left[4\eta'(2|u_x|)|u_x| + \eta(2|u_x|)\right]u_{xx} - p_x\left(x,0\right) + f_1\left(x,0\right) \tag{2.7}$$

where $\eta'(\dot{\gamma}) = \frac{d\eta(\dot{\gamma})}{d\dot{\gamma}}$. For the Power-Law rheology model, $\eta(\dot{\gamma}) = \bar{\kappa}|\dot{\gamma}|^{n-1}$, (2.7) gives the Power-Law Burgers' equation (1.8), which reduces to the classical Burgers' equation (1.5) when $n = 1$,$\bar{\kappa} = \kappa \cdot 2^{n-1}$,and $\kappa = 2\mu$.

2.2 Three Rheology Models

In the following sections, the Cross model[16]: $\eta(\dot{\gamma}) = \eta_\infty + \frac{\eta_0 - \eta_\infty}{1+\bar{\kappa}|\dot{\gamma}|^n}$, the Carreau model[16]: $\eta(\dot{\gamma}) = \eta_\infty + (\eta_o - \eta_\infty)\left(1 + \bar{\kappa}|\dot{\gamma}|^2\right)^{\frac{n}{2}}$,and the Power-Law model[16]: $\eta(\dot{\gamma}) = \bar{\kappa}|\dot{\gamma}|^{n-1}$, are considered and the corresponding traveling wave solutions of (2.6) for these models are solved numerically.

Chapter 3

Traveling Wave Solutions of Burgers' Equation based on the Cross Model

3.1 Derivations of Burgers' Equations for the Cross Model

In this section, we derive traveling wave solutions to the Burger's equation for the Cross model: $\eta(\dot{\gamma}) = \eta_\infty + \frac{\eta_0 - \eta_\infty}{1+\bar{\kappa}|\dot{\gamma}|^n}$. By using (2.6), we have

$$\begin{cases} \rho(u_t + uu_x) = (2\bar{\eta}(u_x)u_x)_x - \bar{\eta}(u_x)u_{xx} \\ \bar{\eta}(u_x) = \eta_\infty + \frac{\eta_0 - \eta_\infty}{1+\bar{\kappa}|u_x|^n}, \bar{\kappa} = (2\kappa)^n \end{cases} \tag{3.1}$$

where we read and calculate the value of κ from reference [2] as in section (3.2). Letting $u(x,t) = u(x-ct) = u(\xi)$ for some constant c. Letting $u'(\xi) = \frac{du}{d\xi}$, then $u_x = u'$, $u_t = -cu'$. Rewriting equation (3.1) in the traveling wave coordinate ξ to yield

$$-\rho c u' + \rho u u' = (2\bar{\eta}(u')u')' - (\int_0^{u'} \bar{\eta}(s)ds)' \tag{3.2}$$

Applying the following boundary conditions to equation (3.1) to get

$$\begin{cases} u(-\infty) = u_l, u'(-\infty) = 0 \\ u(\infty) = u_r, u'(\infty) = 0 \end{cases} \tag{3.3}$$

where u_r and u_l are positive constants. Integrating equation (3.2) to give

$$2\bar{\eta}(u')u' - \int_0^{u'} \bar{\eta}(s)ds = \rho\left(\frac{u^2}{2} - cu\right) + c_1 \tag{3.4}$$

Applying boundary conditions (3.3) to equation (3.4)

$$\begin{cases} c_1 = \rho\frac{u_l u_r}{2} \\ c = \frac{u_l + u_r}{2} \end{cases} \tag{3.5}$$

Substituting equation (3.5) into equation (3.4)

$$2\bar{\eta}(u')u' - \int_0^{u'} \bar{\eta}(s)ds = \rho\left(\frac{u^2}{2} - \frac{u_l + u_r}{2}u\right) + \rho\frac{u_l u_r}{2}$$

$$2\bar{\eta}(u')u' - \int_0^{u'} \bar{\eta}(s)ds = \frac{\rho}{2}\left[u^2 - (u_l + u_r)u + u_l u_r\right]$$

$$2\bar{\eta}(u')u' - \int_0^{u'} \bar{\eta}(s)ds = \frac{\rho}{2}(u - u_l)(u - u_r) \tag{3.6}$$

3.2 Fluid 1 of the Cross Model

Applying the Cross model to equation (3.6). It's a first order implicit ODE that we consider as $F(u', u, \xi) = 0$. Applying the ode15i() function in MATLAB to solve equation (3.6) numerically. We name fluid 1 of the Cross model as the fluid in the seventh row under Cross section in Table 1 in [2]. We read the following statistics $\rho = 26$, $\eta_o = 7.03$, $\eta_\infty = 8.46 \times 10^{-3}$, $n = 0.969$, and $\kappa = 0.195$ from [2]. Equation (3.6) then becomes,

$$\frac{u^2}{2} - \frac{1}{2}u = \left[0.000650769 + \frac{0.540118}{1 + 0.401552|u'|^{0.969}}\right]u' - \int_0^{u'}\left(0.000325385 + \frac{0.270059}{1 + 0.401552|s|^{0.969}}\right)ds$$

$$\begin{aligned}\frac{u^2}{2} - \frac{1}{2}u = &\left[0.000325385 + \frac{0.540118}{1 + 0.401552|u'|^{0.969}}\right]u' \\ &+ \int_0^{u'}\left(\frac{-0.270059}{1 + 0.401552|s|^{0.969}}\right)ds\end{aligned} \tag{3.7}$$

We find a numerical solution for fluid 1 with integral term of the Cross model as the following.

Applying the following boundary conditions

$$\begin{cases} u_l = 1 \\ u_r = 0 \end{cases}$$

and taking initial condition as

$$u(0) = \frac{u_l + u_r}{2} = \frac{1+0}{2} = \frac{1}{2} \tag{3.8}$$

Substituting equation (3.8) into equation (3.7)

$$\begin{aligned} -\frac{1}{8} = &\left[0.000325385 + \frac{0.540118}{1 + 0.401552|u'(0)|^{0.969}}\right] u'(0) \\ &+ \int_0^{u'(0)} \left(\frac{-0.270059}{1 + 0.401552|s|^{0.969}}\right) ds \end{aligned} \tag{3.9}$$

Since $u'(0) < 0, |u'(0)| = -u'(0)$,

$$\begin{aligned} -\frac{1}{8} = &\left\{0.000325385 + \frac{0.540118}{1 + 0.401552\left[-u'(0)\right]^{0.969}}\right\} u'(0) \\ &+ \int_0^{u'(0)} \left\{\frac{-0.270059}{1 + 0.401552(-s)^{0.969}}\right\} ds \end{aligned}$$

$$\begin{aligned} &\left\{0.000325385 + \frac{0.540118}{1 + 0.401552\left[-u'(0)\right]^{0.969}}\right\} u'(0) \\ &+ \int_0^{u'(0)} \left\{\frac{-0.270059}{1 + 0.401552(-s)^{0.969}}\right\} ds + \frac{1}{8} = 0 \end{aligned} \tag{3.10}$$

Assuming $x = -u'(0)$ and giving the following definition

$$\begin{aligned} f(x) = &-0.000325385x - \frac{0.540118x}{1 + 0.401552x^{0.969}} \\ &+ \int_0^{-x} \frac{-0.270059}{1 + 0.401552\left(-s\right)^{0.969}} ds + \frac{1}{8} \end{aligned} \tag{3.11}$$

For the integral term,substituting $y = -s$, then $ds = -dy$. When $s = 0$, $y = 0$; and when $s = -x$, $y = x$. The integral term becomes $\int_0^x \left(\frac{0.270059}{1+0.401552y^{0.969}}\right) dy$. Applying Taylor series expansion to the definite integral at $y = 1$ (and confirmed by [33]) to produce

$$\begin{aligned} \int_0^x \left(\frac{0.270059}{1 + 0.401552y^{0.969}}\right) dy = 0.192686(x-1) - 0.026747\left(x-1\right)^2 \\ +0.00522679\left(x-1\right)^3 - 0.0012171\left(x-1\right)^4 + 0.0032857\left(x-1\right)^5 + 0.226205 \end{aligned}$$

Therefore, equation (3.11) becomes

$$f(x) = -0.000325385x - \frac{0.540118x}{1 + 0.401552x^{0.969}} + 0.192686(x-1)$$
$$-0.026747(x-1)^2 + 0.00522679(x-1)^3 - 0.0012171(x-1)^4$$
$$+0.0032857(x-1)^5 + 0.351206$$

Applying the fzero function in MATLAB[29] to solve $f(x) = 0$ to give $x = 0.671428$.

3.2.1 Plots for Fluid 1 of the Cross Model with the Integral Term

So, for fluid 1 with integral term in the Cross model, $u(0) = \frac{1}{2}, u'(0) = -0.671428$. Applying the ode15i() function in MATLAB to plot the wave profile[7]

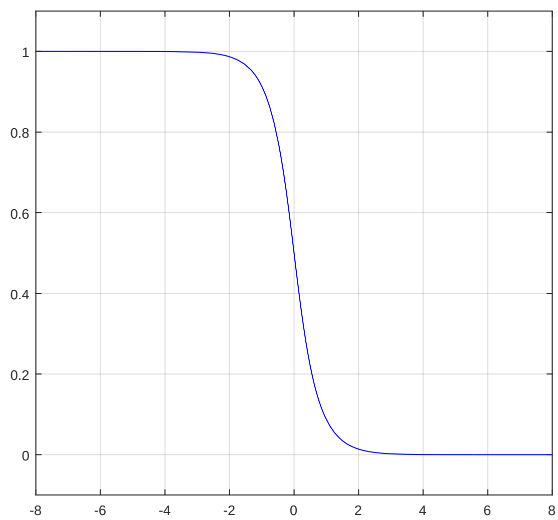

FIGURE 3.1: Wave Profile $u(x)$ for the Cross Model with the Integral Term.

We plot $u'(x)$ as the following

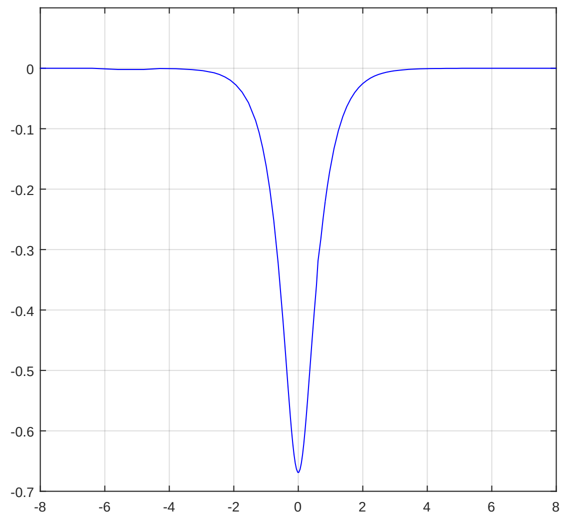

FIGURE 3.2: $u'(x)$ for the Cross Model with the Integral Term.

We plot velocity vectors as the following

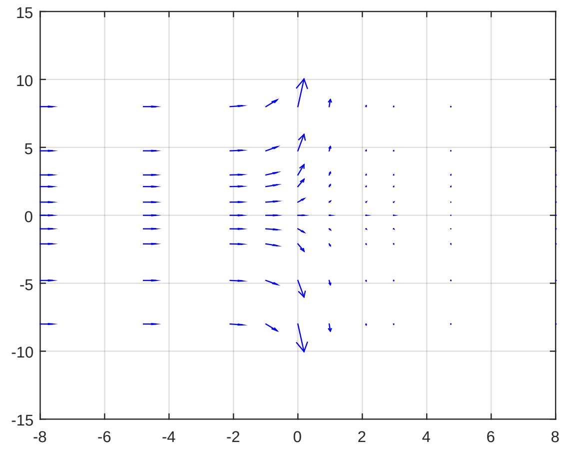

FIGURE 3.3: Velocity Vectors for the Cross Model with the Integral Term.

3.2.2 Plots for Fluid 1 of the Cross Model without the Integral Term

For fluid 1 without the integral term in the Cross model, equation (3.7) is reduced to

$$\frac{u^2}{2} - \frac{1}{2}u = \left[0.000325385 + \frac{0.540118}{1 + 0.401552|u'|^{0.969}}\right] u'$$

with $u(0) = \frac{1}{2}$,$u'(0) = -0.256085$.

Applying the ode15i() function in MATLAB to plot the wave profile[7]

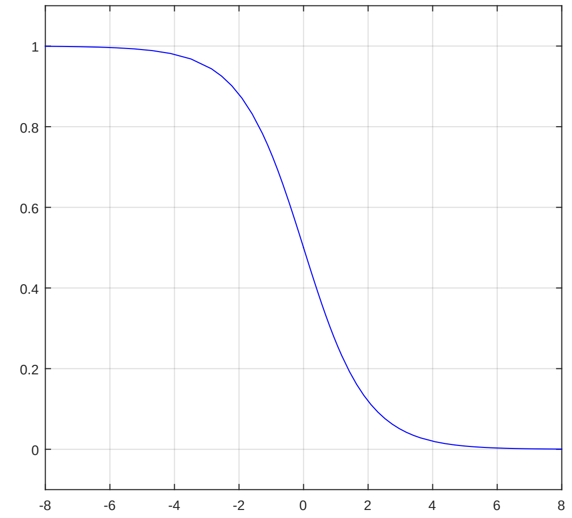

FIGURE 3.4: Wave Profile $u(x)$ for the Cross Model without the Integral Term.

We plot $u'(x)$ as the following

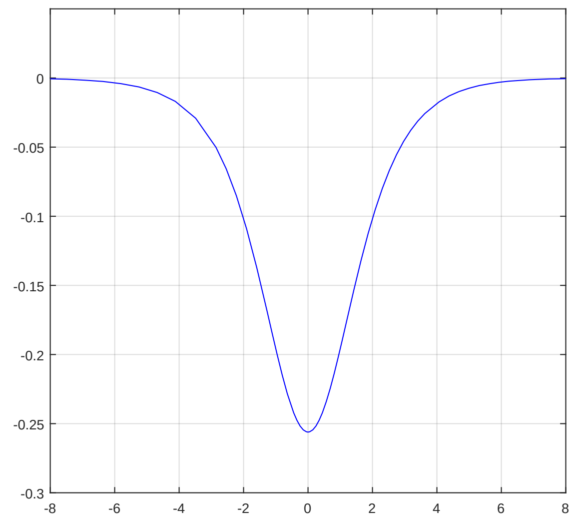

FIGURE 3.5: $u'(x)$ for the Cross Model without the Integral Term.

We plot velocity vectors as the following

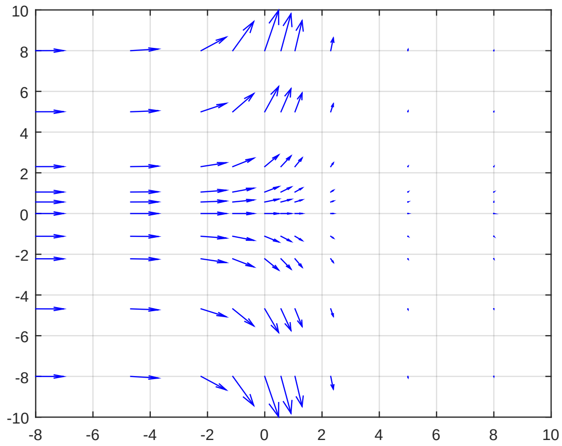

FIGURE 3.6: Velocity Vectors for the Cross Model without the Integral Term.

Chapter 4

Traveling Wave Solutions of Burgers' Equation based on the Carreau Model

4.1 Burgers' Equation for the Carreau Model

The Burgers' equation for the Carreau model is

$$\begin{cases} \rho(u_t + uu_x) = (2\bar{\eta}(u_x)u_x)_x - \bar{\eta}(u_x)u_{xx} \\ \bar{\eta} = \left[\eta_\infty + (\eta_o - \eta_\infty)\left(1 + \bar{K}|u_x|^2\right)^{\frac{n}{2}}\right], \bar{\kappa} = 4\kappa^2 \end{cases} \tag{4.1}$$

Applying the following boundary conditions to equation (4.1)

$$\begin{cases} u(-\infty) = u_l, u'(-\infty) = 0 \\ u(\infty) = u_r, u'(\infty) = 0 \end{cases} \tag{4.2}$$

where u_r and u_l are positive constants.

4.2 Fluid A of the Carreau Model

We name fluid A of the Carreau model as the fluid in the first row under Carreau section in table 1 in [2].
For fluid A of the Carreau model, we read and calculate the following statistics $\eta_0 = 0.0209, \eta_\infty = 0.00249$, $n = 1.61$, $\kappa = 0.576$, and $\rho = 2.74$ from [2].

The procedure in Chapter 3 shall apply mutatis mutandis, then we have

$$\begin{aligned} \frac{u^2}{2} - \frac{1}{2}u = \left[0.000908759 + 0.150737\left(1 + 1.327104\left|u'\right|\right)^2\right]^{0.305} u' \\ + \int_0^{u'} \left[-0.0.0753686\left(1 + 1.327104\left|s\right|\right)^2\right]^{0.305} ds \end{aligned} \tag{4.3}$$

with $u(0) = \frac{1}{2}, u'(0) = -1.073771$. Note: we discard $u'(0) = 3.140661$ because it contradicts with the fact that $u'(0) < 0$; and we discard the $u'(0) = -6.509337$ because it will not make the ode15i() function converge. The Power series expansion of the integral term in equation (4.3) is confirmed by [34].

4.2.1 Plots for Fluid A of the Carreau Model with the Integral Term

Applying the ode15i() function in MATLAB to plot the wave profile[7]

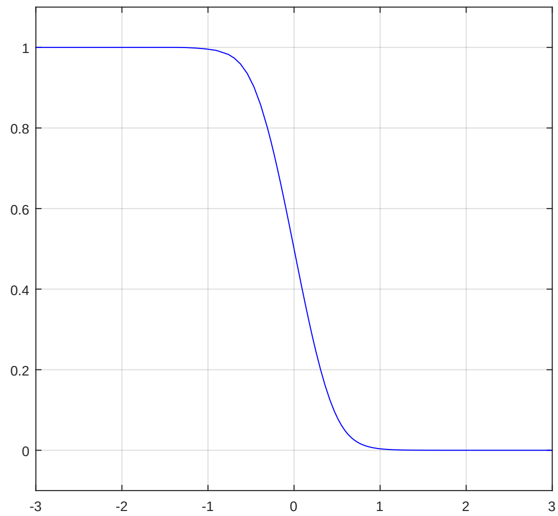

FIGURE 4.1: Wave Profile $u(x)$ for the Carreau Model with the Integral Term.

We plot $u'(x)$ as the following

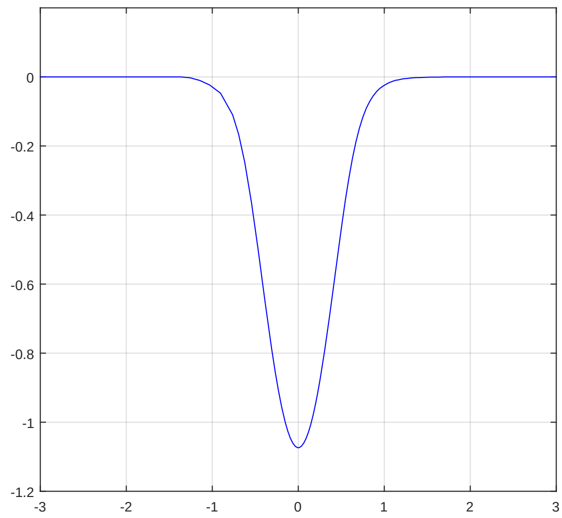

FIGURE 4.2: $u'(x)$ for the Carreau Model with the Integral Term.

We plot velocity vectors as the following

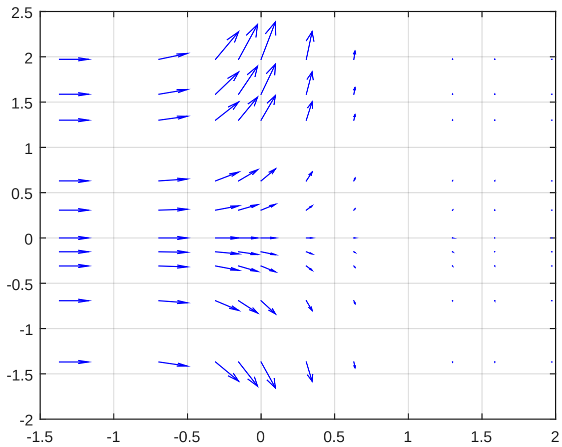

FIGURE 4.3: Velocity Vectors for the Carreau Model with the Integral Term.

4.2.2 Plots for Fluid A of the Carreau Model without the Integral Term

For fluid A without the integral term in the Carreau model,equation (4.3) is reduced to

$$\frac{u^2}{2} - \frac{1}{2}u = \left[0.000908759 + 0.150737\left(1 + 1.327104\left|u'\right|\right)^2\right]^{0.305} u'$$

with $u(0) = \frac{1}{2}$,$u'(0) = -0.706521$.
Apply the ode15i() function to plot the wave profile[7]

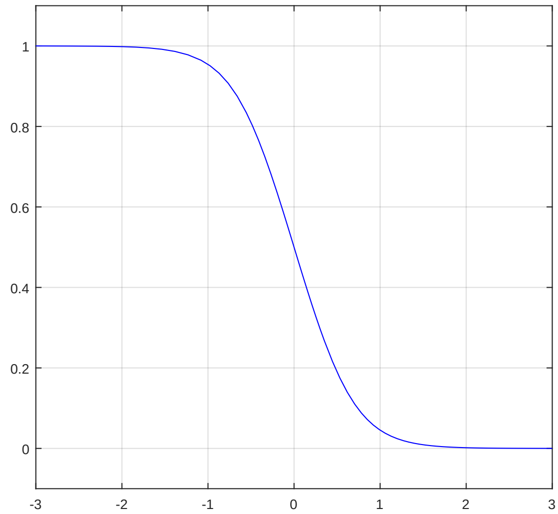

FIGURE 4.4: Wave Profile $u(x)$ for the Carreau Model without the Integral Term.

We plot $u'(x)$ as the following

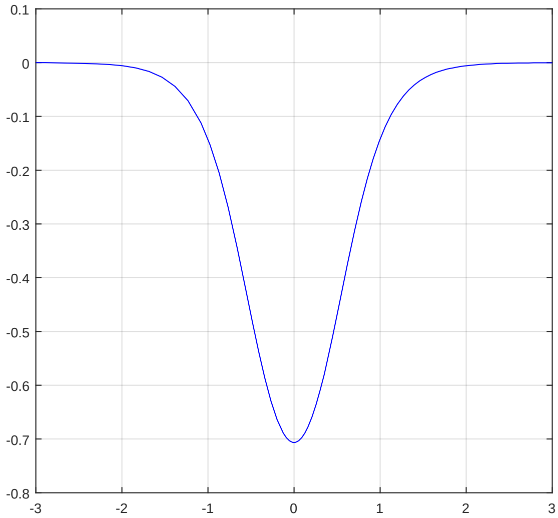

FIGURE 4.5: $u'(x)$ for the Carreau Model without the Integral Term.

We plot velocity vectors as the following

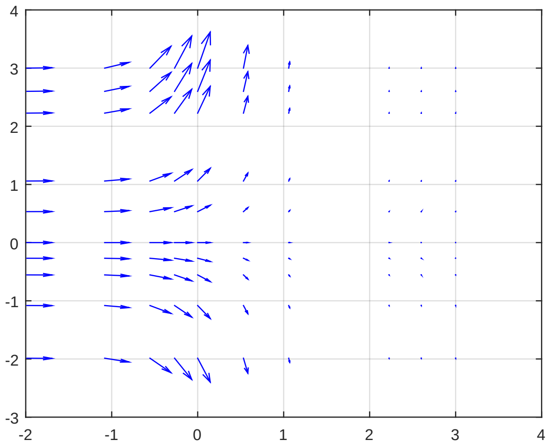

FIGURE 4.6: Velocity Vectors for the Carreau Model without the Integral Term.

Chapter 5

Traveling Wave Solutions of Burgers' Equation based on the Power-Law Model

5.1 Burgers' Equation for the Power-Law Model

The Burgers equation for the Power-Law model is

$$\begin{cases} \rho(u_t + uu_x) = (2\bar{\eta}(u_x)u_x)_x - \bar{\eta}(u_x)u_{xx} \\ \eta\left(u_x\right) = \bar{\kappa}\left|u_x\right|^{n-1}, \bar{\kappa} = \kappa \cdot 2^{n-1} \end{cases} \tag{5.1}$$

Applying the following boundary conditions to equation (3.10),

$$\begin{cases} u(-\infty) = u_l, u(-\infty) = 0 \\ u(\infty) = u_r, u(\infty) = 0 \end{cases} \tag{5.2}$$

where u_r and u_l are positive constants.

5.2 Fluid Mayonnaise of the Power-Law Model

Selecting fluid mayonnaise of the Power-Law rheology model in Table 10.4 from [26]. We then read and calculate the following statistics for mayonnaise of the Power-Law model at 25 °C, $\kappa = 6.4$,and $n = 0.55$ from [26].The density of mayonnaise of the Power-Law model can be calculated as the average of densities of light and traditional mayonnaises as in [31], i.e., $\rho = 955$.

The procedure in Chapter 3 shall apply mutatis mutandis,then we have

$$\frac{u^2}{2} - \frac{u}{2} = 0.00981167 \left|u'\right|^{-0.45} u' - 0.00490584 \int_0^{u'} |s|^{-0.45}\, ds \tag{5.3}$$

with $u(0) = \frac{1}{2}, u'(0) = -7995.484568$. Note: there is no need to apply the Power series expansion to the integral term of the Power-Law model because we do the integration directly.

5.2.1 Plots for Fluid 1 of the Power-Law Model with the Integral Term

Applying the ode15i() function in MATLAB to plot the wave profile[7]

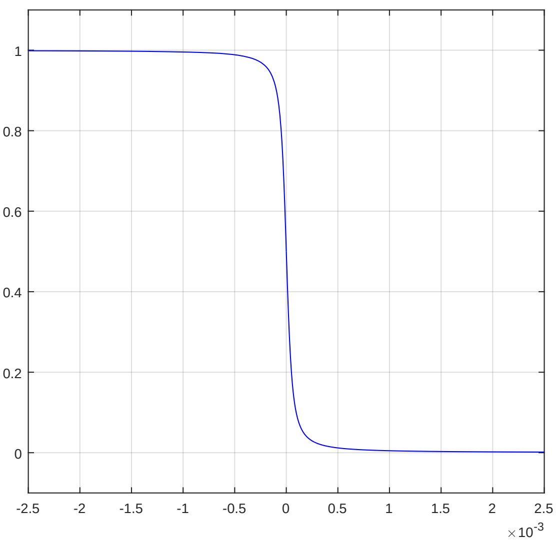

FIGURE 5.1: Wave Profile $u(x)$ for the Power-Law Model with the Integral Term.

We plot $u'(x)$ as the following

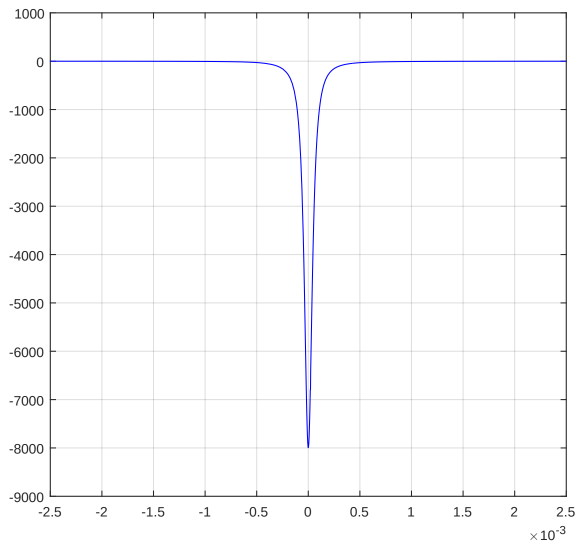

FIGURE 5.2: $u'(x)$ for the Power-Law Model with the Integral Term.

We plot velocity vectors as the following

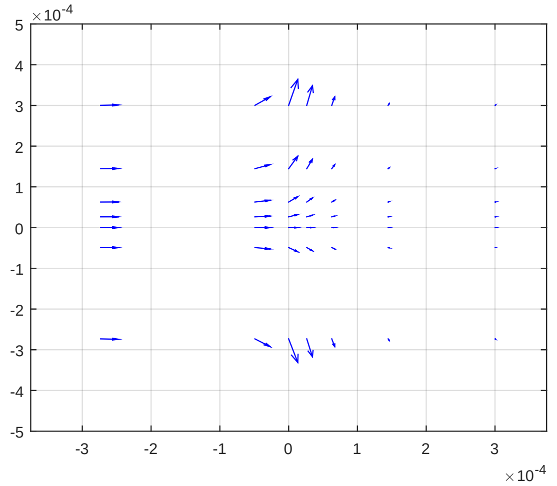

FIGURE 5.3: Velocity Vectors for the Power-Law Model with the Integral Term.

5.2.2 Plots for Fluid 1 of the Power-Law Model without the Integral Term

If without the integral term, equation (5.3) is reduced to

$$\frac{u^2}{2} - \frac{u}{2} = -0.00981167 \left|u'\right|^{0.55}$$

with $u(0) = \frac{1}{2}$,$u'(0) = -102.186775$.
Applying the ode15i() to plot the wave profile[7]

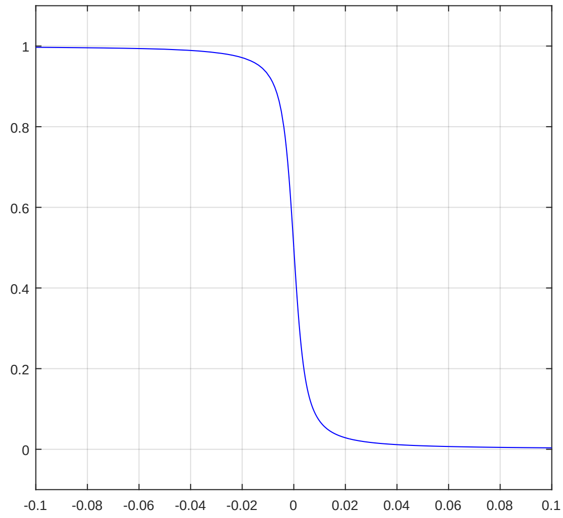

FIGURE 5.4: Wave Profile $u(x)$ for the Power-Law Model without the Integral Term.

We plot $u'(x)$ as the following

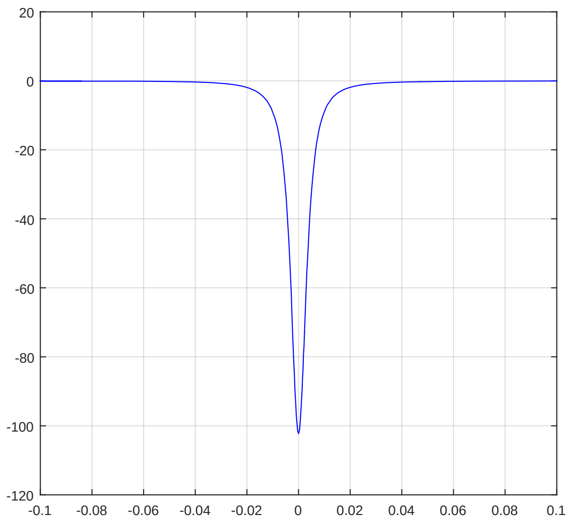

FIGURE 5.5: $u'(x)$ for the Power-Law Model without the Integral Term.

We plot velocity vectors as the following

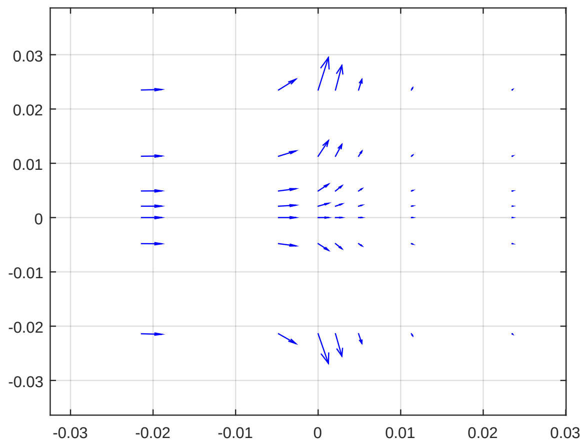

FIGURE 5.6: Velocity Vectors for the Power-Law Model without the Integral Term.

Chapter 6

Existence and Uniqueness of Solutions to the Traveling Wave Equations

6.1 Existence and Uniqueness of Solutions

The equations (3.2), (3.3), (4.1), (4.2), (5.1), and (5.2) can be written in the following form

$$F(u'(\xi), u(\xi), \xi) = \int_0^{u'(\xi)} \eta(s)ds - 2\eta(u'(\xi))u'(\xi) + au^2(\xi) + bu(\xi) + c \tag{6.1}$$

where $\eta(u'(\xi))$ is the apparent viscosity of the fluids and $a = \frac{\rho}{2}, b = -\rho\frac{u_l+u_r}{2}, c = \frac{u_l u_r}{2}$ are the constants.

If without the integral term, equation (6.1) is reduced to

$$F(u'(\xi), u(\xi), \xi) = -2\eta(u'(\xi))u'(\xi) + au^2(\xi) + bu(\xi) + c \tag{6.2}$$

where $\eta(u'(\xi))$ is the apparent viscosity of the fluids and $a = \frac{\rho}{2}, b = -\rho\frac{u_l+u_r}{2}, c = \frac{u_l u_r}{2}$ are the constants. According to the Peano theorem in the implicit case[10, pp.28-31], and Uniqueness in the implicit case[10, pp. 44-47] in Murray and Miller's book on existence theorem on ODE, we need to prove the followings:

(1)$F(u'(\xi), u(\xi), \xi)$ of the three real variables $u'(\xi), u(\xi), \xi$ is defined and continuous on an open region $\mathcal{U}$ of 3-dimensional Euclidean space. Here, $\mathcal{U}$ is determined by the domain of the function.

(2)$\frac{\partial F}{\partial u'}$ exists and is continuous on $\mathcal{U}$.

(3)$\frac{\partial F}{\partial u}$ exists and is continuous on $\mathcal{U}$.

(4)there exists a set of values $((u'(0), u(0), \xi(0)))$ in $\mathcal{U}$ such that

$$F(u'(\xi), u(\xi), \xi) = 0$$

and

$$J = \frac{\partial F}{\partial u'} \neq 0$$

at this point.

Additionally, $\frac{\partial F}{\partial \xi} = 0$ is satisfied automatically for three models. So, in the following sections, we only consider u' and u in F.

6.2 Existence and Uniqueness of Solutions for the Cross Model with the Integral Term

Substituting second expression of (3.1) into equation (kumquat) to produce

$$F(u', u) = \int_0^{u'} \left(\eta_\infty + \frac{\eta_0 - \eta_\infty}{1 + \bar{\kappa} |s|^n} \right) ds - 2 \left(\eta_\infty + \frac{\eta_0 - \eta_\infty}{1 + \bar{\kappa} |u'|^n} \right) + \frac{\rho}{2} u^2 - \frac{\rho (u_l + u_r)}{2} u + \frac{u_l u_r}{2} \tag{6.3}$$

Rearranging terms in equation (6.3)) to give

$$F(u', u) = \int_0^{u'} \left(\frac{\eta_0 - \eta_\infty}{1 + \bar{\kappa} |s|^n} \right) ds - \left[\eta_\infty + \frac{2(\eta_0 - \eta_\infty)}{1 + \bar{\kappa} |u'|^n} \right] u' + \frac{\rho}{2} u^2 - \frac{\rho (u_l + u_r)}{2} u + \frac{u_l u_r}{2} \tag{6.4}$$

6.2.1 Continuity of $\frac{\partial F}{\partial u'}$

Since $u' < 0$, taking partial derivative of equation (6.4) with respect to u' gives

$$\frac{\partial F(u', u)}{\partial u'} = \frac{\eta_0 - \eta_\infty}{1 + \bar{\kappa} |u'|^n} - \eta_\infty - 2(\eta_0 - \eta_\infty) \left[\frac{(1 + \bar{\kappa} |u'|^n) - u' \cdot n \cdot \bar{\kappa} |u'|^{n-1} \cdot (-1)}{(1 + \bar{\kappa} |u'|^n)^2} \right]$$

Since $-u' = |u'|$,

$$\frac{\partial F}{\partial u'} = \frac{-\eta_\infty (1 + \bar{\kappa} |u'|^n)^2 - (\eta_0 - \eta_\infty)(1 + \bar{\kappa} |u'|^n) + 2n(\eta_0 - \eta_\infty) \bar{\kappa} |u'|^n}{(1 + \bar{\kappa} |u'|^n)^2} \tag{6.5}$$

Plugging the statistics for fluid 1 from Chapter 3 into equation (6.5),

$$\frac{\partial F}{\partial u'} = \frac{-0.00136412\,|u'|^{1.938} + 2.637909\,|u'|^{0.969} - 7.03}{\left(1 + 0.401552\,|u'|^{0.969}\right)^2} \tag{6.6}$$

At the point $(u'(0), u(0)) = \left(-0.671429, \frac{1}{2}, 0\right)$, equation (6.6) becomes

$$\frac{\partial F}{\partial u'}\left(u'(0), u(0), 0\right) = -3.713258 \neq 0$$

6.2.2 Continuity of $\frac{\partial F}{\partial u}$

Taking partial derivative of equation (6.4) with respect to u gives

$$\frac{\partial F}{\partial u} = 26u - 13 \tag{6.7}$$

At the point $(u'(0), u(0)) = \left(-0.671429, \frac{1}{2}\right)$, equation (6.7) becomes

$$\frac{\partial F}{\partial u}\left(u'(0), u(0), 0\right) = 0$$

6.3 Existence and Uniqueness of Solutions for the Cross Model without the Integral Term

Substituting second expression of (3.1) into equation (6.2) to produce

$$F(u', u) = -2\left[\eta_\infty + \frac{\eta_0 - \eta_\infty}{1 + \bar{\kappa}\,|u'|^n}\right]u' + \frac{\rho}{2}u^2 - \frac{\rho\,(u_l + u_r)}{2}u + \frac{u_l u_r}{2} \tag{6.8}$$

6.3.1 Continuity of $\frac{\partial F}{\partial u'}$

Since $u' < 0$, taking partial derivative of equation (6.8) with respect to u' gives

$$\frac{\partial F(u', u)}{\partial u'} = -2\eta_\infty - 2\,(\eta_0 - \eta_\infty)\left[\frac{(1 + \bar{\kappa}\,|u'|^n) - u' n\bar{\kappa}\,|u'|^{n-1}(-1)}{(1 + \bar{\kappa}\,|u'|^n)^2}\right]$$

Since $-u' = |u'|$,

$$\frac{\partial F(u', u)}{\partial u'} = -2\eta_\infty - 2\,(\eta_0 - \eta_\infty)\left[\frac{1 + (1-n)\,\bar{\kappa}\,|u'|^n}{(1 + \bar{\kappa}\,|u'|^n)^2}\right] \tag{6.9}$$

Plugging the statistics for fluid 1 from Chapter 3 into equation (6.9),

$$\frac{\partial F\left(u',u\right)}{\partial u'}=\frac{-0.00272825\left|u'\right|^{1.938}-0.0577977\left|u'\right|^{0.969}-14.06}{\left(1+0.401552\left|u'\right|^{0.969}\right)^{2}} \tag{6.10}$$

Since $|u'|>0$, $\frac{\partial F}{\partial u'}<0$. So, $\frac{\partial F}{\partial u'}\neq 0$.
At the point $\left(u'\left(0\right),u\left(0\right)\right)=\left(-0.256085,\frac{1}{2}\right)$, equation (6.10) becomes

$$\frac{\partial F}{\partial u'}\left(u'\left(0\right),u\left(0\right),0\right)=-11.4806\neq 0$$

6.3.2 Continuity of $\frac{\partial F}{\partial u}$

Taking partial derivative of equation (6.8) with respect to u gives

$$\frac{\partial F}{\partial u}=\rho u-\frac{\rho\left(u_l+u_r\right)}{2} \tag{6.11}$$

For the chosen fluid 1 in Chapter 3, $\rho=26$, $u_l=1$, and $u_r=0$,then the equation (6.11) becomes,

$$\frac{\partial F}{\partial u}=26u-13 \tag{6.12}$$

At the point $\left(u'\left(0\right),u\left(0\right)\right)=\left(-0.256085,\frac{1}{2}\right)$, equation (6.12) becomes

$$\frac{\partial F}{\partial u}\left(u'\left(0\right),u\left(0\right),0\right)=0$$

6.4 Existence and Uniqueness of Solutions for the Carreau Model with the Integral Term

Substituting the second expression from equation (4.1) into equation (6.1) to yield

$$\begin{aligned}F(u',u)&=\int_0^{u'}\left[\eta_\infty+\left(\eta_0-\eta_\infty\right)\left(1+\bar{\kappa}\left|s\right|^2\right)^{\frac{n-1}{2}}\right]ds\\&-2\left[\eta_\infty+\left(\eta_0-\eta_\infty\right)\left(1+\bar{\kappa}\left|u'\right|^2\right)^{\frac{n-1}{2}}\right]u'+\frac{\rho}{2}u^2-\frac{\rho\left(u_l+u_r\right)}{2}u+\frac{u_lu_r}{2}\end{aligned} \tag{6.13}$$

Rearranging terms in equation (6.13) to give

$$\begin{aligned}F\left(u',u\right)&=\int_0^{u'}\left[\left(\eta_0-\eta_\infty\right)\left(1+\bar{\kappa}\left|s\right|^2\right)^{\frac{n-1}{2}}\right]ds\\&-\left[\eta_\infty+2\left(\eta_0-\eta_\infty\right)\left(1+\bar{\kappa}\left|u'\right|^2\right)^{\frac{n-1}{2}}\right]u'+\frac{\rho}{2}u^2-\frac{\rho\left(u_l+u_r\right)}{2}u+\frac{u_lu_r}{2}\end{aligned} \tag{6.14}$$

6.4.1 Continuity of $\frac{\partial F}{\partial u'}$

Since $u' < 0$, taking partial derivative of equation (6.14) with respect to u' gives

$$\begin{aligned}\frac{\partial F}{\partial u'} = (\eta_0 - \eta_\infty)\left(1 + \bar{\kappa}\left|u'\right|^2\right)^{\frac{n-1}{2}} - \eta_\infty \\ -2\left(\eta_0 - \eta_\infty\right)\left[\left(1 + \bar{\kappa}\left|u'\right|^2\right)^{\frac{n-1}{2}} + u' \cdot \left(\frac{n-1}{2}\right)\left(1 + \bar{\kappa}\left|u'\right|^2\right)^{\frac{n-3}{2}} \cdot 2\bar{\kappa}\left|u'\right| \cdot (-1)\right]\end{aligned} \tag{6.15}$$

$$\frac{\partial F}{\partial u'} = \frac{-\eta_\infty\left(1 + \bar{\kappa}\left|u'\right|^2\right)^{\frac{3-n}{2}} - (\eta_0 - \eta_\infty)\left(1 + \bar{\kappa}\left|u'\right|^2\right) - (n-1)\,\bar{\kappa}\left|u'\right|^2}{\left(1 + \bar{\kappa}\left|u'\right|^2\right)^{\frac{3-n}{2}}} \tag{6.16}$$

Plugging the statistics for the chosen fluid A from Chapter 4 into equation (6.16),

$$\frac{\partial F}{\partial u'} = \frac{-0.00249\left(1 + 1.327104\left|u'\right|^2\right)^{0.695} - 0.20651 - 1.083593\left|u'\right|^2}{\left(1 + 1.327104\left|u'\right|^2\right)^{0.695}} \tag{6.17}$$

At the point $(u'(0), u(0)) = (-1.073711, \frac{1}{2})$, equation (6.17) becomes

$$\frac{\partial F}{\partial u'}(u'(0), u(0), 0) = -0.766183 \neq 0$$

6.4.2 Continuity of $\frac{\partial F}{\partial u}$

Taking partial derivative of equation (6.14) with respect to u gives

$$\frac{\partial F}{\partial u} = \rho u - \frac{\rho\left(u_l + u_r\right)}{2} \tag{6.18}$$

Plugging the statistics for the chosen fluid A from Chapter 4 into equation (6.18) to give

$$\frac{\partial F}{\partial u} = 2.74u - 1.37 \tag{6.19}$$

At the point $(u'(0), u(0)) = (-1.073711, \frac{1}{2})$, equation (6.19) becomes

$$\frac{\partial F}{\partial u}(u'(0), u(0), 0) = 0$$

6.5 Existence and Uniqueness of Solutions for the Carreau Model without the Integral Term

Substituting the second expression from equation (4.1) into equation (6.2) to yield

$$F(u,u) = -2\left[\eta_\infty + (\eta_0 - \eta_\infty)\left(1 + \bar{\kappa}\left|u'\right|^2\right)^{\frac{n-1}{2}}\right]u' + \frac{\rho}{2}u^2 \\ -\frac{\rho\left(u_l + u_r\right)}{2}u + \frac{u_l u_r}{2} \tag{6.20}$$

6.5.1 Continuity of $\frac{\partial F}{\partial u'}$

Since $u' < 0$, taking partial derivative of equation (6.20 with respect to u' gives

$$\frac{\partial F\left(u',u\right)}{\partial u'} = -2\eta_\infty - 2\left(\eta_0 - \eta_\infty\right)\left[\left(1 + \bar{\kappa}\left|u'\right|^2\right)^{\frac{n-1}{2}} + u'\left(\frac{n-1}{2}\right)\left(1 + \bar{\kappa}\left|u'\right|^2\right)^{\frac{n-3}{2}} \cdot 2\bar{\kappa}\left|u'\right|(-1)\right]$$

Since $-u' = |u'|$,

$$\frac{\partial F\left(u',u\right)}{\partial u'} = -2\eta_\infty - 2\left(\eta_0 - \eta_\infty\right) \cdot \\ \left[\left(1 + \bar{\kappa}\left|u'\right|^2\right)^{\frac{n-1}{2}} + (n-1)\,\bar{\kappa}\left|u'\right|^2\left(1 + \bar{\kappa}\left|u'\right|^2\right)^{\frac{n-3}{2}}\right] \tag{6.21}$$

Plugging the statistics for the chosen fluid A from Chapter 4 into equation (6.21),

$$\frac{\partial F\left(u',u\right)}{\partial u'} = \frac{-0.882473\left|u'\right|^2 - 0.00498\left(1 + 1.327104\left|u'\right|^2\right)^{0.695} - 0.41302}{\left(1 + 1.327104\left|u'\right|^2\right)^{0.695}} \tag{6.22}$$

Since $|u'| > 0$, $\frac{\partial F}{\partial u'}$ is always negative.So, $\frac{\partial F}{\partial u'} \neq 0$.
At the point $(u'(0), u(0)) = (-0.706521, \frac{1}{2})$, equation (6.22) becomes

$$\frac{\partial F}{\partial u'}(u'(0), u(0), 0) = -0.00498 \neq 0$$

6.5.2 Continuity of $\frac{\partial F}{\partial u}$

Taking partial derivative of equation (6.20) with respect to u gives

$$\frac{\partial F}{\partial u} = \rho u - \frac{\rho\left(u_l + u_r\right)}{2} \tag{6.23}$$

For the chosen fluid A in Chapter 4, $\rho = 2.74$, $u_l = 1$, and $u_r = 0$,then equation (6.23) becomes

$$\frac{\partial F}{\partial u} = 2.74u - 1.37 \tag{6.24}$$

At the point $(u'(0), u(0)) = (-0.706521, \frac{1}{2})$, equation (6.24) becomes

$$\frac{\partial F}{\partial u}(u'(0), u(0), 0) = 0$$

6.6 Existence and Uniqueness of Solutions for the Power-Law Model with the Integral Term

Substituting the second expression from equation (5.1) into equation (6.1) to give

$$\begin{aligned} F(u', u) = \int_0^{u')} \bar{\kappa} \left|s\right|^{n-1} ds - 2\left[\bar{\kappa} \left|u'\right|^{n-1}\right] u' + \frac{\rho}{2} u^2 \\ - \frac{\rho\left(u_l + u_r\right)}{2} u + \frac{u_l u_r}{2} \end{aligned} \tag{6.25}$$

6.6.1 Continuity of $\frac{\partial F}{\partial u'}$

Since $(u')^n$ is undefined when $u' < 0$, taking partial derivative of equation (6.25) with respect to u' gives

$$\frac{\partial F\left(u', u\right)}{\partial u'} = \frac{\bar{\kappa}}{n}\left(-n\left|u'\right|^{n-1}\right) - 2\bar{\kappa}\left[-\left(n-1\right)\left|u'\right|^{n-2} u' + \left|u'\right|^{n-1}\right]$$

Since $-u' = |u'|$,

$$\frac{\partial F\left(u', u\right)}{\partial u'} = \bar{\kappa}\left|u'\right|^{n-1}\left(-1 + 2n\right) \tag{6.26}$$

For the chosen fluid mayonnaise from Chapter 5, $\bar{\kappa} = 0.00490584$, $n = 0.55$, so equation (6.26) becomes

$$\frac{\partial F\left(u', u\right)}{\partial u'} = 0.00490584\left|u'\right|^{-0.45}(0.10)$$

$$\frac{\partial F\left(u', u\right)}{\partial u'} = 0.000490584\left|u'\right|^{-0.45} \neq 0 \tag{6.27}$$

At the point $(u'(0), u(0)) = (-7995.484568, \frac{1}{2})$, equation (6.27) becomes

$$\frac{\partial F}{\partial u'}(u'(0), u(0), 0) = 0.0000085987$$

6.6.2 Continuity of $\frac{\partial F}{\partial u}$

Taking partial derivative of equation (6.25) with respect to u gives

$$\frac{\partial F}{\partial u} = \rho u - \frac{\rho \left(u_l + u_r\right)}{2} \tag{6.28}$$

For the chosen fluid mayonnaise in Chapter 5, $\rho = 955$, $u_l = 1$, and $u_r = 0$,

$$\frac{\partial F}{\partial u} = 955u - 477.5 \tag{6.29}$$

At the point $(u'(0), u(0)) = (-7995.484568, \frac{1}{2})$, equation (6.29) becomes

$$\frac{\partial F}{\partial u}(u'(0), u(0), 0) = 0$$

6.7 Existence and Uniqueness of Solutions for the Power-Law Model without the Integral Term

Substituting the second expression from equation (5.1) into equation (6.2) to give

$$F(u, u) = -2\left[\bar{\kappa}\left|u'\right|^{n-1}\right]u' + \frac{\rho}{2}u^2 - \frac{\rho\left(u_l + u_r\right)}{2}u + \frac{u_l u_r}{2} \tag{6.30}$$

6.7.1 Continuity of $\frac{\partial F}{\partial u'}$

Since $u' < 0$, taking partial derivative of equation (6.30) with respect to u' gives

$$\frac{\partial F\left(u', u\right)}{\partial u'} = -2\bar{\kappa}\left[(n-1)\left|u'\right|^{n-2}(-1)\,u' + \left|u'\right|^{n-1}\right]$$

Since $-u' = |u'|$,

$$\frac{\partial F\left(u', u\right)}{\partial u'} = -2\bar{\kappa}\left[(n-1)\left|u'\right|^{n-1} + \left|u'\right|^{n-1}\right]$$

$$\frac{\partial F\left(u', u\right)}{\partial u'} = -2n\bar{\kappa}\left|u'\right|^{n-1} \tag{6.31}$$

Plugging the statistics for the chosen fluid mayonnaise from Chapter 5 into equation (6.31),

$$\frac{\partial F\left(u', u\right)}{\partial u'} = \frac{-5.153581}{|u'|^{0.45}} \tag{6.32}$$

Since $|u'| > 0$, $\frac{\partial F}{\partial u'}$ is always negative. So, $\frac{\partial F}{\partial u'} \neq 0$.
At the point $(u'(0), u(0)) = (-102.186775, \frac{1}{2})$,equation (6.32) becomes

$$\frac{\partial F}{\partial u'}(u'(0), u(0), 0) = -0.642512$$

6.7.2 Continuity of $\frac{\partial F}{\partial u}$

Taking partial derivative of equation (6.30) with respect to u gives

$$\frac{\partial F}{\partial u} = \rho u - \frac{\rho\,(u_l + u_r)}{2} \tag{6.33}$$

For the chosen fluid mayonnaise in Chapter 5, $\rho = 955$, $u_l = 1$, and $u_r = 0$,then equation (6.33) becomes

$$\frac{\partial F}{\partial u} = 955u - 477.5 \tag{6.34}$$

At the point $(u'(0), u(0)) = (-102.186775, \frac{1}{2})$,equation (6.34) becomes

$$\frac{\partial F}{\partial u}(u'(0), u(0), 0) = 0$$

6.8 Theorem on Existence and Uniqueness of Solutions for all Three Models

Theorem 6.1. *There exists a unique solution to each of the equations in sections (6.2)-(6.7) by the Peano theorem.*

Chapter 7

The Order of Thickness of the Transition Layers

7.1 Derivations and Formulas

The transition layer thickness or shock thickness of the kink waves and the associated solitons can be computed by using the first order derivative $\frac{du}{d\xi}|_{\xi=0}$ for the three industrial fluids and comparisons are made as indicated by the tables 7.1, 7.2, and 7.3 [5],[6]. We make three tables based on the the numerical solutions of the three industrial fluids as the following

We use δ to denote the thickness of the transition layer[5],[6]. We apply the Taylor series expansion to yield [5],[6]

$$u_l - u_r \approx u(-\frac{\delta}{2}) - u(\frac{\delta}{2}) = -\delta \frac{du}{d\xi}(0) + 0(\delta^2)$$

Therefore, we have $\delta = -\frac{u_l - u_r}{u'(0)} = -\frac{1}{u'(0)}$. For each of the three fluids, the maximum strain ε_{11} is calculated. These maximum strain ε_{11} occurs at center of the kink wave and the center of the soliton.

7.2 Tables and Discussion

We assign the value with the integral term as a reference in the calculations of relative error and percent error.

TABLE 7.1: Shock Thickness and Maximum Strain ε_{11} for Fluid 1 of the Cross Model

Name of Fluid	Value of $u'(0)$	Thickness	Maximum Strain ε_{11}
Fluid 1 with the integral term	-0.671429	1.48936	-6.15670
Fluid 1 without the integral term	-0.256085	3.90495	-2.97648
Relative error	0.415344	2.41559	3.18022
Percent error	-61.8597%	162.1898%	-51.6546%

TABLE 7.2: Shock Thickness and Maximum Strain ε_{11} for the Fluid A of the Carreau Model

Name of Fluid	Value of $u'(0)$	Thickness	Maximum Strain ε_{11}
Fluid A with the Integral Term	-1.07377	0.931297	-0.845399
Fluid A without the Integral Term	-0.706521	1.41539	-0.436619
Relative error	0.367249	0.484093	0.40878
Percent error	-34.2018%	51.9805%	-48.3535%

TABLE 7.3: Shock Thickness and Maximum Strain ε_{11} for the Fluid Mayonnaise of the Power-Law Model

Name of Fluid	Value of $u'(0)$	Thickness	Maximum Strain ε_{11}
Mayonnaise with the Integral Term	-7995.485	0.000125071	-961.275
Mayonnaise without the Integral Term	-102.187	0.00978600	-87.3876
Relative error	7893.298	0.00966093	873.887
Percent error	-98.7219%	7724.36%	-90.9092%

Since the Burgers' equation comes with by assuming the shear stress $\tau_{12} = 0$ which is not realistic in modeling real fluid flows, we did not assume the shear stress $\tau_{12} = 0$ in the derivations of traveling wave equations with the integral term in equation (3.2). The differences are significant as indicated by tables 7.1, 7.2, and 7.3.

Chapter 8

Conclusion

In this thesis, generalized Burgers' equations for some common non-Newtonian fluid flows are derived from the general the Navier-Stokes equations under planer symmetry and incompressibility conditions. Traveling wave solution of these equations are obtained numerically for several commonly encountered fluids with industrial rheological data. Profiles of the transition layers of the traveling waves are demonstrated. A first-order approximation of the thickness of the transition layer or thickness of the shocks are also computed numerically. The first-order implicit integral differential equation is numerically solved by the MATLAB built-in ode15i() function. Existence and uniqueness of the solutions to each of the three traveling wave equations for the three non-Newtonian fluid models are proved by using the Peano Theorems for implicit first order ODEs. It is demonstrated that the velocity are kink waves while the strains are solitons through numerical solutions.

Appendix A

MATLAB Codes

A.1 MATLAB Codes for fluid 1 of the Cross Model with the Integral Term

The M-file for fluid 1 of the Cross model with the integral term to find x for $f(x) = 0$ by using the fzero function is named as

```
cross_integral_term_fezro.m
```

and the codes are

```
function y=f(x)
y=(-0.000325385-0.540118/(1+0.401552*(x^0.969)))*x+0.192686*(x-1)
-0.026747*(x-1)^2+0.00522679*(x-1)^3-0.0012171*(x-1)^4
+0.00032857*(x-1)^5+0.351505;
```

The $u'(0) = -x$ found in the fzero function becomes an input in the ode15i() function. The M-fiel for the ode15i() function for the Cross model with the integral term to plot the wave profile $u(x)$ is named as

```
cross_model_integral_term_code.m
```

and the codes are

```
f1=@(t,u,ud)[(0.000325385+(0.540118/((1+0.401552*(abs(ud)^0.969)))))*ud
-0.192686*(ud+1)-0.026747*(ud+1)^2-0.00522679*(ud+1)^3-0.0012171*(ud+1)^4
-0.00032857*(ud+1)^5+0.226205-0.5*(u^2)+0.5*u];
u0=[0.5]; ud0=[-0.671429]; u0F=[1]; ud0F=[];
[u0,ud0]=decic(f1,0,u0,u0F,ud0,ud0F);
r1=ode15i(f1,[0,8],u0,ud0);
r2=ode15i(f1,[0,-8],u0,ud0);
plot(r1.x,r1.y,'b',r2.x,r2.y,'b');
grid
```

Then we modify the codes above a bit and click on the "RUN" button to display the value of $r1$ in MATLAB's command window as the following

```
f1=@(t,u,ud)[(0.000325385+(0.540118/((1+0.401552*(abs(ud)^0.969)))))*ud
-0.192686*(ud+1)-0.026747*(ud+1)^2-0.00522679*(ud+1)^3-0.0012171*(ud+1)^4
-0.00032857*(ud+1)^5+0.226205-0.5*(u^2)+0.5*u];
u0=[0.5]; ud0=[-0.671429]; u0F=[1]; ud0F=[];
[u0,ud0]=decic(f1,0,u0,u0F,ud0,ud0F);
r1=ode15i(f1,[0,8],u0,ud0)
```

In MATLAB's command window, we enter $x1 = r1.x$ to display the values of $x1$, enter $y1 = r1.x$ to display the values of $y1$, and enter $u1 = r.y1$ to display the values of $u1$. The similar operations on $r2$ shall apply mutatis mutandis. We record the values of $x1$ and $x2$ as the values of x, record values of $y1$ and $y2$ as values of y, and record the values of $u1$ and $u2$ as the values of u. Next, we apply the following codes in MATLAB's command window to find the values of $u'(x)$

```
ud=fzero(@(ud) [(0.000325385+(0.540118/((1+0.401552*(abs(ud)^0.969)))))*ud
-0.192686*(ud+1)-0.026747*(ud+1)^2-0.00522679*(ud+1)^3-0.0012171*(ud+1)^4
-0.00032857*(ud+1)^5+0.226205-0.5*(u^2)+0.5*u],0.5)
```

by replacing varible u by a value of u from the recorded data, for instance, 0.4874 and press the "Enter" button to get $u'(0.4874)$. We continue the computations until we get all values of u'. If a negative value of u' occurs, we can simply change the initial guess at the end of ud expression from 0.5 to -0.5 and press the "Enter" button. If the result does not converge, we can simply change the initial guess at the end of ud expression to a smaller value, for instance, 0.05, and press the "Enter" button. We use the values of u' for the plots of $u'(x)$ and velocity vectors. Similar operations for finding values of u and u' shall apply mutatis mutandis for the other fluids.
The M-file for $u'(x)$ of the Cross model with the integral term is named as

```
cross_integral_term_ud.m
```

and the codes are

```
x=[-8.0000 -7.1928 -6.3928 -5.5928 -4.7928 -4.2946 -3.7963 -3.2980
-2.9566 -2.6152 -2.4445 -2.2738 -2.1030 -1.9323 -1.7426 -1.5442
-1.3236 -1.2134 -1.1031 -0.9928 -0.8826 -0.7601 -0.6239 -0.4727
-0.3970 -0.3214 -0.2458 -0.2080 -0.1702 -0.1323 -0.0945 -0.0567
-0.0189 0 0.0189 0.0567 0.0945 0.1323 0.1702 0.2080 0.2458 0.2836
0.3592 0.4273 0.4954 0.5634 0.6115 0.6996 0.7676 0.8357 0.9038
0.9718 1.1079 1.2441 1.3802 1.5027 1.6252 1.7478 1.8703 1.9928
2.1153 2.2378 2.3603 2.4829 2.6054 2.7279 2.8504 2.9729 3.2180
3.4218 3.6052 3.7684 3.9316 4.0949 4.2581 4.4213 4.5845 4.7477
4.9110 5.0742 5.2374 5.4006 5.5639 5.7271 5.8903 6.0535 6.2168
6.5106 6.8044 7.0982 7.6858 8.0000];
ud=[0 0 0 -0.002 -0.002 -0.0004 -0.0007 -0.0022 -0.0040 -0.0074
-0.0103 -0.0144 -0.0199 -0.0277 -0.0395 -0.0570 -0.0864 -0.1067
```

```
-0.1319 -0.1626 -0.2003 -0.2520 -0.3229 -0.4187 -0.4715 -0.5253
-0.5769 -0.6004 -0.6215 -0.6394 -0.6535 -0.6633 -0.6684 -0.6690
-0.6684 -0.6633 -0.6535 -0.6394 -0.6215 -0.6004 -0.5769 -0.5517
-0.4983 -0.4498 -0.4030 -0.3592 -0.3189 -0.2822 -0.2494 -0.2202
-0.1942 -0.1712 -0.1328 -0.1030 -0.0799 -0.0635 -0.0507 -0.0403
-0.0321 -0.0256 -0.0205 -0.0162 -0.0129 -0.0103 -0.0083 -0.0066
-0.0053 -0.0042 -0.0028 -0.0018 -0.0013 -0.0009 -0.0007 -0.0005
-0.0004 -0.0004 -0.0002 -0.0002 -0.0002 0.0000 0.0000 0.0000
0.0000 0.0000 0.0000 0.0000 0.0000 0.0000 0.0000 0.0000 0.0000
0.0000];

figure
plot(x,ud,'b')
grid
```

The M-file for the velocity vectors of the Cross model with the integral term is named as

```
cross_model_integral_term_quiver.m
```

and the codes are

```
x=[-8.0000 -4.7928 -2.1030 -0.9928 0 0.9718 2.1153 2.9729
4.7477 8.0000];
y=[-8.0000 -4.7928 -2.1030 -0.9928 0 0.9718 2.1153 2.9729
4.7477 8.0000];
u=[1 0.9999 0.9892 0.9125 0.5000 0.0921 0.0111 0.0023 0.0001 0.0000;
1 0.9999 0.9892 0.9125 0.5000 0.0921 0.0111 0.0023 0.0001 0.0000;
1 0.9999 0.9892 0.9125 0.5000 0.0921 0.0111 0.0023 0.0001 0.0000;
1 0.9999 0.9892 0.9125 0.5000 0.0921 0.0111 0.0023 0.0001 0.0000;
1 0.9999 0.9892 0.9125 0.5000 0.0921 0.0111 0.0023 0.0001 0.0000;
1 0.9999 0.9892 0.9125 0.5000 0.0921 0.0111 0.0023 0.0001 0.0000;
1 0.9999 0.9892 0.9125 0.5000 0.0921 0.0111 0.0023 0.0001 0.0000;
1 0.9999 0.9892 0.9125 0.5000 0.0921 0.0111 0.0023 0.0001 0.0000;
1 0.9999 0.9892 0.9125 0.5000 0.0921 0.0111 0.0023 0.0001 0.0000;
1 0.9999 0.9892 0.9125 0.5000 0.0921 0.0111 0.0023 0.0001 0.0000];
v=[0 -0.0016 -0.1592 -1.3008 -5.352 -1.3696 -0.164 -0.0336 -0.0016
 0; 0 -0.0009586 -0.09538 -0.7793 -3.2064 -0.8205 -0.09825 -0.02013
-0.0009586 0;0 -0.0004206 -0.04185 -0.3419 -1.4069 -0.3600 -0.04311
-0.008833 -0.0004206 0;0 -0.0001986 -0.01976 -0.1614 -0.6642 -0.1700
-0.02035 -0.004170 -0.0001986 0;0 0 0 0 0 0 0 0 0 0; 0 0.0001944
0.01934 0.1580 0.6501 0.1664 0.01992 0.004082 0.0001944 0; 0 0.0004231
0.04209 0.3439 1.4151 0.3621 0.04336 0.008884 0.0004231 0; 0 0.0005946
0.05916 0.4834 1.9889 0.5090 0.06094 0.01249 0.0005946 0; 0 0.0009495
0.09448 0.7720 3.1762 0.8128 0.09733 0.01994 0.0009495 0; 0 0.0016 0.
1592 1.3008 5.352 1.3696 0.164 0.0336 0.0016 0];

figure
quiver(x,y,u,v,'b')
grid
```

A.2 MATLAB Codes for Fluid 1 of the Cross Model without the Integral Term

The M-file for fluid 1 of the Cross model without the integral term to find x for $f(x) = 0$ by using the fzero function is named as

```
cross_fluid_1_fzero.m
```

and the codes are

```
function y=f(x)
y=(-0.000325385-0.540118/(1+0.401552*(x^0.969)))*x+0.125;
```

The $u'(0) = -x$ found in the fzero function becomes an input in the ode15i() function. The M -file for the ode15i() function for the Cross model without the integral term to plot the wave profile $u(x)$ is named as

```
cross_mode_code.m
```

and the codes are

```
f1=@(t,u,ud)[(0.000325385+(0.540118/((1+0.401552*(abs(ud)^0.969)))))*ud
-0.5*(u^2)+0.5*u];
u0=[0.5]; ud0=[-0.256085]; u0F=[1]; ud0F=[];
[u0,ud0]=decic(f1,0,u0,u0F,ud0,ud0F);
r1=ode15i(f1,[0,8],u0,ud0);
r2=ode15i(f1,[0,-8],u0,ud0);
plot(r1.x,r1.y,'b',r2.x,r2.y,'b');
grid
```

The M-file for codes for $u'(x)$ of the Cross model without the integral term is named as

```
cross_ud.m
```

and the codes are

```
x=[-8.0000 -7.4902 -6.9285 -6.3667 -5.8050 -5.2432 -4.6815 -4.1197
-3.4874 -2.8552 -2.5390 -2.2229 -1.9067 -1.5906 -1.2744 -1.1163
-0.9583 -0.8002 -0.6421 -0.4445 -0.3458 -0.2470 -0.1482 -0.0494 0
0.0494 0.1482 0.2470 0.3458 0.4445 0.5669 0.6893 0.8116 0.9340 1.0563
1.1787 1.4234 1.6436 1.8639 2.0841 2.3044 2.5246 2.7449 2.9651 3.1854
3.4056 3.6258 4.0663 4.3769 4.6875 4.9981 5.3087 5.6193 5.9298 6.2404
6.5510 6.8616 7.1722 7.4828 7.7934 8.0000];
ud=[-0.0006 -0.0009 -0.0016 -0.0025 -0.0041 -0.0065 -0.0105 -0.0169
-0.0291 -0.0502 -0.0657 -0.0852 -0.1091 -0.1372 -0.1683 -0.1843 -0.2000
-0.2149 -0.2284 -0.2422 -0.2475 -0.2517 -0.2545 -0.2559 -0.2561 -0.2559
-0.2545 -0.2517 -0.2475 -0.2422 -0.2340 -0.2245 -0.2138 -0.2022 -0.1902
-0.1778 -0.1532 -0.1321 -0.1126 -0.0953 -0.0800 -0.0668 -0.0555 -0.0459
-0.0379 -0.0312 -0.0257 -0.0173 -0.0130 -0.0098 -0.0074 -0.0055 -0.0042
-0.0031 -0.0023 -0.0018 -0.0013 -0.0010 -0.0007 -0.0006 -0.0005];
```

```
figure
plot(x,ud,'b')
grid
```

The M-file for codes for the velocity vectors of the Cross model without the integral term is named as

```
cross_model_quiver.m
```

and the codes are

```
x=[-8.0000 -4.6815 -2.2229 -1.1163 0 0.5669 1.0563 2.3044 4.9981
8.0000];
y=[-8.0000 -4.6815 -2.2229 -1.1163 0 0.5669 1.0563 2.3044 4.9981
8.0000];
u=[0.9994 0.9886 0.9015 0.7553 0.5000 0.3598 0.2556 0.0920 0.0080
0.0005; 0.9994 0.9886 0.9015 0.7553 0.5000 0.3598 0.2556 0.0920 0.0080
0.0005; 0.9994 0.9886 0.9015 0.7553 0.5000 0.3598 0.2556 0.0920 0.0080
0.0005; 0.9994 0.9886 0.9015 0.7553 0.5000 0.3598 0.2556 0.0920 0.0080
0.0005; 0.9994 0.9886 0.9015 0.7553 0.5000 0.3598 0.2556 0.0920 0.0080
0.0005; 0.9994 0.9886 0.9015 0.7553 0.5000 0.3598 0.2556 0.0920 0.0080
0.0005; 0.9994 0.9886 0.9015 0.7553 0.5000 0.3598 0.2556 0.0920 0.0080
0.0005; 0.9994 0.9886 0.9015 0.7553 0.5000 0.3598 0.2556 0.0920 0.0080
0.0005; 0.9994 0.9886 0.9015 0.7553 0.5000 0.3598 0.2556 0.0920 0.0080
0.0005; 0.9994 0.9886 0.9015 0.7553 0.5000 0.3598 0.2556 0.0920 0.0080
0.0005];
v=[-0.0048 -0.084 -0.6816 -1.4744 -2.0488 -1.872 -1.5216 -0.64 -0.0592
-0.004; -0.002809 -0.04916 -0.3989 -0.8628 -1.1989 -1.0955 -0.8904
-0.3745 -0.03464 -0.002341; -0.001334 -0.02334 -0.1894 -0.4097 -0.5693
-0.5202 -0.4228 -0.1778 -0.01645 -0.001111; -0.0006698 -0.01172
-0.09511 -0.2057 -0.2859 -0.2612 -0.2123 -0.08930 -0.008261
-0.0005582; 0 0 0 0 0 0 0 0 0 0; 0.0003401 0.005952 0.04830 0.1045
0.1452 0.1327 0.1078 0.04535 0.004195 0.002835; 0.0006338 0.01109
0.09000 0.1947 0.2705 0.2472 0.2009 0.08450 0.007817
0.0005282; 0.001383 0.02420 0.1963 0.4247 0.5902 0.5392 0.4383 0.1844
0.01705 0.001152; 0.002999 0.05248 0.4258 0.9211 1.2800 1.1696 0.9506
0.3998 0.03699 0.002499; 0.0048 0.084 0.6816 1.4744 2.0488 1.872 1.5216
0.64 0.0592 0.004];

figure
quiver(x,y,u,v,'b')
grid
```

A.3 MATLAB Codes for Fluid 1 of the Carreau Model with the Integral Term

The M-file for fluid A of the Carreau model with the integral term to find x for $f(x) = 0$ by using the fzero function is named as

```
carreau_fluid_A_integral_term_fzero.m
```

and the codes are

```
function y=f(x)
function y=f(x)
y=(-0.000908759-0.150737*((1+1.327104*(x^2))^(0.305)))*x+0.0975145*(x-1)
+0.01696*(x-1)^2+0.00117207*(x-1)^3-0.0011952*(x-1)^4+0.000595404*(x-1)^5
+0.208517;
```

The $u'(0) = -x$ found in the fzero function becomes an input in the ode15i() function. The M-file for the ode15i() function for the Carreau model with integral term to plot the wave profile $u(x)$ is named as

```
carreau_integral_term_fluid_A_fzero.m
```

and the codes are

```
f1=@(t,u,ud)[(0.000908759+0.150737*((1+1.327104*(abs(ud))^2)^(0.305)))*ud
-0.0975145*(ud+1)+0.01696*(ud+1)^2-0.00117207*(ud+1)^3-0.0011952*(ud+1)^4
-0.000595404*(ud+1)^5+0.0835172-0.5*(u^2)+0.5*u];
u0=[0.5]; ud0=[--1.073771]; u0F=[1]; ud0F=[];
[u0,ud0]=decic(f1,0,u0,u0F,ud0,ud0F);
r1=ode15i(f1,[0,3],u0,ud0);
r2=ode15i(f1,[0,-3],u0,ud0);
plot(r1.x,r1.y,'b',r2.x,r2.y,'b');
grid
```

The M-file for $u'(x)$ of the Carreau model with the integral term is named as

```
carreau_integral_term_ud.m
```

and the codes are

```
x=[-3.0000 -2.6745 -2.3745 -2.0745 -1.7745 -1.5718 -1.3691 -1.2564
-1.1438 -1.0312 -0.9044 -0.7634 -0.6929 -0.6225 -0.5441 -0.4658
-0.3875 -0.3092 -0.2701 -0.2309 -0.1918 -0.1526 -0.1233 -0.0940
-0.0647 -0.0353 -0.0118 0 0.0118 0.0353 0.0625 0.0897 0.1169 0.1441
0.1712 0.1984 0.2256 0.2528 0.3071 0.3615 0.4158 0.4702 0.5101
0.5501 0.5900 0.6300 0.6699 0.7098 0.7498 0.7897 0.8297 0.8696
0.9096 0.9495 0.9895 1.0294 1.0653 1.1013 1.1337 1.1660 1.1984
1.2307 1.2656 1.3005 1.3354 1.3703 1.4052 1.4750 1.5341 1.5868
1.6395 1.6921 1.7622 1.8322 1.9022 1.9722 2.0422 2.1123 2.1823
2.3223 2.4419 2.5614 2.6810 2.9200 3.0000];
ud=[0 0 0 0 0 0 0 -0.0026 -0.0104 -0.0234 -0.0471 -0.1099 -0.1670
-0.2474 -0.3644 -0.5023 -0.6494 -0.7885 -0.8516 -0.9083 -0.9579
-0.9994 -1.0249 -1.0451 -1.0601 -1.0697 -1.0733 -1.0738 -1.0733
-1.0697 -1.0610 -1.0476 -1.0298 -1.0073 -0.9806 -0.9498 -0.9152
-0.8769 -0.7915 -0.6965 -0.5960 -0.4945 -0.4216 -0.3522 -0.2908
-0.2355 -0.1885 -0.1493 -0.1173 -0.0913 -0.0713 -0.0554 -0.0427
-0.0330 -0.0259 -0.0201 -0.0156 -0.0123 -0.0098 -0.0085 -0.0065
```

```
-0.0052 -0.0046 -0.0033 -0.0026 -0.0020 -0.0020 -0.0013 -0.0007
-0.0007 -0.0007 0 0 0 0 0 0 0 0 0 0 0 0 0 0];

figure
plot(x,ud,'b')
grid
```

The M-file for the velocity vectors of the Carreau model with the integral term is named as

```
carreau_model_integral_term_quiver.m
```

and the codes are

```
x=[-1.3691 -0.6929 -0.3092 -0.1526 0 0.3071 0.6300 1.3005 1.5868 1.9722];
y=[-1.3691 -0.6929 -0.3092 -0.1526 0 0.3071 0.6300 1.3005 1.5868 1.9722];
u=[1.0000 0.9732 0.8004 0.6592 0.5000 0.2010 0.0389 0.0005 0.0001
0.0000; 1.0000 0.9732 0.8004 0.6592 0.5000 0.2010 0.0389 0.0005
0.0001 0.0000; 1.0000 0.9732 0.8004 0.6592 0.5000 0.2010 0.0389
0.0005 0.0001 0.0000; 1.0000 0.9732 0.8004 0.6592 0.5000 0.2010
0.0389 0.0005 0.0001 0.0000;1.0000 0.9732 0.8004 0.6592 0.5000
0.2010 0.0389 0.0005 0.0001 0.0000;1.0000 0.9732 0.8004 0.6592
0.5000 0.2010 0.0389 0.0005 0.0001 0.0000; 1.0000 0.9732 0.8004
0.6592 0.5000 0.2010 0.0389 0.0005 0.0001 0.0000; 1.0000 0.9732
0.8004 0.6592 0.5000 0.2010 0.0389 0.0005 0.0001 0.0000; 1.0000
0.9732 0.8004 0.6592 0.5000 0.2010 0.0389 0.0005 0.0001 0.0000; 1.0000
0.9732 0.8004 0.6592 0.5000 0.2010 0.0389 0.0005 0.0001 0.0000];
v=[0 -0.2286 -1.0795 -1.3683 -1.4701 -1.0836 -0.3224 -0.004518
-0.0009584 0; 0 -0.1157 -0.5464 -0.6925 -0.7440 -0.5484 -0.1632
-0.002287 -0.0004850 0; 0 -0.05164 -0.2438 -0.3090 -0.3320 -0.2447
-0.07282 -0.001020 -0.0002164 0; 0 -0.02548 -0.1203 -0.1525 -0.1639
-0.1208 -0.03594 -0.0005036 -0.0001068 0; 0 0 0 0 0 0 0 0 0 0; 0 0.05129
0.2421 0.3069 0.3298 0.2431 0.07232 0.001013 0.002150 0; 0 0.1052 0.4968
0.6296 0.6765 0.4986 0.1484 0.002079 0.000441 0; 0 0.2172 1.0254 1.2997
1.3965 1.0293 0.3063 0.004292 0.0009104 0; 0 0.2650 1.2512 1.5858 1.7039
1.2560 0.3737 0.005236 0.001111 0; 0 0.3294 1.5551 1.9710 2.1177 1.5610
0.4645 0.006508 0.001381 0];

figure
quiver(x,y,u,v,'b')
grid
```

A.4 MATLAB Codes for Fluid A of the Carreau Model without the Integral Term

The M-file for fluid A of the Carreau model without the integral term to find x for $f(x) = 0$ by using the fzero function is named as

```
carreau_fluid_A_fzero
```

and the codes are

```
function y=f(x)
y=(-0.000908759-0.150737*((1+1.327104*(x^2))^(0.305)))*x+0.125;
```

The $u'(0) = -x$ found in the fzero function becomes an input in the ode15i() function. The M-file for the ode15i() function for the Carreau model without integral term to plot the wave profile $u(x)$ is names as

```
carreau_model_integral_term.m
```

and the codes are

```
f1=@(t,u,ud)[(0.000908759+0.150737*((1+1.327104*(abs(ud))^2)^(0.305)))*ud
-0.5*(u^2)+0.5*u];
u0=[0.5]; ud0=[-0.706521]; u0F=[1]; ud0F=[];
[u0,ud0]=decic(f1,0,u0,u0F,ud0,ud0F);
r1=ode15i(f1,[0,3],u0,ud0);
r2=ode15i(f1,[0,-3],u0,ud0);
plot(r1.x,r1.y,'b',r2.x,r2.y,'b');
grid
```

The M-file for codes for $u'(x)$ of the Carreau model without the integral term is named as

```
carreau_ud.m
```

and the codes are

```
x=[-3.0000 -2.8890 -2.5890 -2.2890 -2.1380 -1.9871 -1.8361 -1.6852
-1.5343 -1.3833 -1.2324 -1.0815 -0.9762 -0.8709 -0.7656 -0.6603
-0.5550 -0.4834 -0.4118 -0.3402 -0.2686 -0.1969 -0.1253 -0.0895
-0.0537 -0.0179 0 0.0179 0.0537 0.0895 0.1253 0.1611 0.2088 0.2564
0.3040 0.3516 0.4469 0.5326 0.6183 0.7041 0.7812 0.8507 0.9201
0.9896 1.0590 1.1297 1.2005 1.2712 1.3349 1.3985 1.4622 1.5259
1.5895 1.6532 1.7169 1.7805 1.8442 1.9079 1.9715 2.0352 2.0988
2.1625 2.2262 2.2898 2.3574 2.4182 2.4790 2.5398 2.6006 2.6614
2.7222 2.7830 2.8439 2.9047 2.9655 3.0000];
ud=[0 0 -0.0010 -0.0023 -0.0036 -0.0059 -0.0099 -0.0164 -0.0271
-0.0442 -0.0708 -0.1120 -0.1528 -0.2047 -0.2692 -0.3447 -0.4267
-0.4828 -0.5368 -0.5863 -0.6293 -0.6640 -0.6890 -0.6975 -0.7033
-0.7062 -0.7065 -0.7062 -0.7033 -0.6975 -0.6890 -0.6777 -0.6588
-0.6356 -0.6086 -0.5794 -0.5101 -0.4435 -0.3761 -0.3119 -0.2587
-0.2160 -0.1785 -0.1464 -0.1192 -0.0962 -0.0774 -0.0620 -0.0506
-0.0413 -0.0336 -0.0275 -0.0223 -0.0180 -0.0148 -0.0118 -0.0099
-0.0079 -0.0063 -0.0053 -0.0043 -0.0033 -0.0026 -0.0023 -0.0016
-0.0013 -0.0013 -0.0010 -0.0007 -0.0007 -0.0007 -0.0003 -0.0003
-0.0003 -0.0003 -0.0003];

figure
plot(x,ud,'b')
grid
```

The M-file for the velocity vectors of the Carreau model without the integral term is named as

```
carreau_model_quiver.m
```

and the codes are

```
x=[-1.9871 -1.0815 -0.5550 -0.2686 0 0.5326 1.0590 2.2262 2.6006
3.0000];
y=[-1.9871 -1.0815 -0.5550 -0.2686 0 0.5326 1.0590 2.2262 2.6006
3.0000];
u=[0.9982 0.9646 0.8344 0.6818 0.5000 0.1749 0.0378 0.0008 0.0002
0.0001; 0.9982 0.9646 0.8344 0.6818 0.5000 0.1749 0.0378 0.0008
0.0002 0.0001; 0.9982 0.9646 0.8344 0.6818 0.5000 0.1749 0.0378
0.0008 0.0002 0.0001; 0.9982 0.9646 0.8344 0.6818 0.5000 0.1749
0.0378 0.0008 0.0002 0.0001; 0.9982 0.9646 0.8344 0.6818 0.5000
0.1749 0.0378 0.0008 0.0002 0.0001; 0.9982 0.9646 0.8344 0.6818
0.5000 0.1749 0.0378 0.0008 0.0002 0.0001; 0.9982 0.9646 0.8344
0.6818 0.5000 0.1749 0.0378 0.0008 0.0002 0.0001; 0.9982 0.9646
0.8344 0.6818 0.5000 0.1749 0.0378 0.0008 0.0002 0.0001; 0.9982
0.9646 0.8344 0.6818 0.5000 0.1749 0.0378 0.0008 0.0002 0.0001; 0.9982
0.9646 0.8344 0.6818 0.5000 0.1749 0.0378 0.0008 0.0002 0.0001];
v=[-0.01172 -0.2226 -0.8479 -1.2505 -1.4039 -0.8813 -0.2369 -0.005166
-0.001391 -0.0005961; -0.006381 -0.1211 -0.4615 -0.6806 -0.7641 -0.4796
-0.1289 -0.002812 -0.0007571 -0.0003245; -0.003275 -0.06216 -0.2368
-0.3493 -0.3921 -0.2461 -0.06616 -0.001443 -0.0003885
-0.0001665; -0.001585 -0.03008 -0.1146 -0.1690 -0.1898 -0.1191
-0.03202 -0.0006984 -0.0001880 -0.00008058; 0 0 0 0 0 0 0
0 0 0; 0.003142 0.05965 0.2273 0.3352 0.3763 0.2362 0.06349
0.001385 0.0003728 0.0001598; 0.006248 0.1186 0.4519 0.6664
0.7482 0.4697 0.1262 0.002753 0.0007413 0.0003177; 0.01313 0.2493
0.9499 1.4009 1.5728 0.9873 0.2654 0.005788 0.001558 0.0006679; 0.01534
0.2913 1.1097 1.6366 1.8373 1.1534 0.3100 0.006762 0.001820
0.0007802; 0.0177 0.336 1.2801 1.8879 2.1195 1.3305 0.3576 0.0078
0.0021 0.0009];

figure
quiver(x,y,u,v,'b')
grid
```

A.5 MATLAB Codes for Fluid Mayonnaise of the Power-Law Model with the Integral Term

The M-file for fluid mayonnaise of the Power-Law model with the integral term to find x for $f(x) = 0$ by using the fzero function is named as

```
power_law_mayonnaise_integral_term_fzero.m
```

and the codes are

```
function y=f(x)
y=-0.000891960*(x^0.55)+0.125;
```

The $u'(0) = -x$ found in the fzero function becomes an input in the ode15i() function. The M-file for the ode15i() function for the Power-Law model with integral term to plot the wave profile $u(x)$ is named as

```
power_law_model_integral_term_code.m
```

and the codes are

```
f1=@(t,u,ud)[-0.000891960*(abs(ud)^(0.55))-0.5*(u^2)+0.5*u];
u0=[0.5]; ud0=[-7995.484568]; u0F=[1]; ud0F=[];
[u0,ud0]=decic(f1,0,u0,u0F,ud0,ud0F);
r1=ode15i(f1,[0,0.0025],u0,ud0);
r2=ode15i(f1,[0,-0.0025],u0,ud0);
plot(r1.x,r1.y,'b',r2.x,r2.y,'b');
grid
```

The M-file for $u'(x)$ of the Power-Law model with the integral term is named as

```
power_law_integral_term_ud.m
```

and the codes are

```
x=[-0.00250000 -0.00230473 -0.00205473 -0.00180473 -0.00155473
-0.00135150 -0.00114827 -0.000945046 -0.000843432 -0.000741818
-0.000640204 -0.000527299 -0.000470847 -0.000414394 -0.000357942
-0.000329716 -0.000301490 -0.000273264 -0.000245038 -0.000213675
-0.000194135 -0.000174596 -0.000155056 -0.000135516 -0.000115976
-0.000105121 -0.0000942655 -0.0000834101 -0.0000725547
-0.0000616992 -0.0000490430 -0.0000427149 -0.0000363867
-0.0000300586 -0.0000237305 -0.0000205664 -0.0000174023
-0.0000142383 -0.0000110742 -0.00000791016 -0.00000474610
-0.00000158203 0 0.00000158203 0.00000474610 0.00000791016
0.0000107578 0.0000133207 0.0000156273 0.0000177033 0.0000195716
0.0000214399 0.0000231215 0.0000248030 0.0000263163 0.0000278297
0.0000291917 0.0000305537 0.0000319158 0.0000332778 0.0000346398
0.0000360019 0.0000387259 0.0000414500 0.0000468981 0.0000523462
0.0000577943 0.0000626976 0.0000676008 0.0000725041 0.0000774074
0.0000831060 0.0000888046 0.0000945032 0.000100202 0.000107594
0.000114987 0.000122380 0.000129772 0.000137165 0.000144557
0.000151950 0.000165257 0.000177233 0.000189209 0.000201185
0.000213161 0.000225137 0.000237642 0.000250146 0.000262651
0.000275156 0.000287660 0.000300165 0.000325175 0.000350184
0.000375193 0.000400203 0.000425212 0.000450222 0.000475231
0.000500240 0.000525250 0.000550259 0.000575269 0.000600278
0.000645295 0.000690312 0.000735329 0.000780346 0.000825363
0.000870380 0.000915400 0.000960413 0.00100543 0.00105045 0.00114048
0.00122098 0.00130148 0.00138198 0.00146248 0.00154298 0.00162348
0.00170398 0.00178449 0.00186499 0.00197261 0.00208023 0.00218785
0.00229548 0.00240310 0.00250000];
```

```
ud=[-0.601221 -0.704480 -0.909760 -1.25282 -1.76409 -2.45379 -3.74990
-5.87134 -7.68406 -10.3654 -14.6221 -24.4231 -32.7142 -45.8444
-66.2407 -80.8612 -100.588 -127.200 -164.573 -227.100 -281.579
-356.066 -462.877 -619.163 -856.454 -1043.26 -1288.38 -1611.61
-2046.50 -2639.64 -3589.38 -4183.14 -4853.76 -5579.15 -6319.04
-6675.22 -7009.65 -7311.29 -7569.03 -7771.60 -7913.15 -7986.20
-7995.48 -7986.20 -7913.15 -7771.60 -7591.21 -7391.50 -7186.03
-6983.77 -6790.24 -6790.24 -6401.88 -6211.93 -6037.83 -5863.90
-5706.04 -5549.75 -5394.29 -5238.33 -5083.77 -4930.95 -4632.87
-4346.68 -3814.37 -3340.95 -2925.00 -2598.73 -2313.40 -2064.33
-1846.22 -1627.78 -1441.09 -1281.21 -1143.57 -992.375 -866.363
-760.957 -672.189 -596.810 -532.364 -477.041 -395.968 -338.556
-292.255 -254.349 -223.059 -196.830 -173.793 -154.374 -137.885
-123.790 -111.657 -101.135 -83.9159 -70.5794 -60.0769 -51.6717
-44.8530 -39.2490 -34.5952 -30.6957 -27.4045 -24.6045 -22.1927
-20.1057 -17.0085 -14.5609 -12.5973 -10.9950 -9.67387 -8.56609
-7.62889 -6.83144 -6.14920 -5.56129 -4.61719 -3.94340 -3.40891
-2.97286 -2.61333 -2.31353 -2.06119 -1.84658 -1.66267 -1.50370
-1.32367 -1.17336 -1.04676 -0.93906 -0.846762 -0.774456];

figure
plot(x,ud,'b')
grid
```

The M-file for the velocity vectors of the Power-Law model with the integral term is named as

```
power_law_model_integral_term_quiver.m
```

and the codes are

```
x=[-0.002500 -0.001555 -0.0002733 -0.00004904 0 0.00002632 0.00006270
0.0001446 0.0003002 0.0006453 0.001382 0.002500];
y=[-0.002500 -0.001555 -0.0002733 -0.00004904 0 0.00002632 0.00006270
0.0001446 0.0003002 0.0006453 0.001382 0.002500];
u=[0.9987 0.9976 0.9737 0.8378 0.5000 0.3108 0.1605 0.05993 0.02313
0.008550 0.003259 0.001552;  0.9987 0.9976 0.9737 0.8378 0.5000 0.3108
0.1605 0.05993 0.02313 0.008550 0.003259 0.001552; 0.9987 0.9976 0.9737
0.8378 0.5000 0.3108 0.1605 0.05993 0.02313 0.008550 0.003259
0.001552; 0.9987 0.9976 0.9737 0.8378 0.5000 0.3108 0.1605 0.05993
0.02313 0.008550 0.003259 0.001552; 0.9987 0.9976 0.9737 0.8378
0.5000 0.3108 0.1605 0.05993 0.02313 0.008550 0.003259 0.001552; 0.9987
0.9976 0.9737 0.8378 0.5000 0.3108 0.1605 0.05993 0.02313 0.008550
0.003259 0.001552; 0.9987 0.9976 0.9737 0.8378 0.5000 0.3108 0.1605
0.05993 0.02313 0.008550 0.003259 0.001552; 0.9987 0.9976 0.9737 0.8378
0.5000 0.3108 0.1605 0.05993 0.02313 0.008550 0.003259 0.001552; 0.9987
0.9976 0.9737 0.8378 0.5000 0.3108 0.1605 0.05993 0.02313 0.008550
0.003259 0.001552; 0.9987 0.9976 0.9737 0.8378 0.5000 0.3108 0.1605
0.05993 0.02313 0.008550 0.003259 0.001552; 0.9987 0.9976 0.9737 0.8378
0.5000 0.3108 0.1605 0.05993 0.02313 0.008550 0.003259 0.001552; 0.9987
0.9976 0.9737 0.8378 0.5000 0.3108 0.1605 0.05993 0.02313 0.008550
0.003259 0.001552];
v=[-0.001503 -0.004410 -0.318 -6.5991 -19.9887 -15.0946 -6.4968
-1.3309 -0.2528 -0.04252 -0.007432 -0.001936; -0.0009347 -0.002743
```

```
-0.1978 -4.1039 -12.4308 -9.3872 -4.0403 -0.8277 -0.1572 -0.02644
-0.004622 -0.001204; -0.0001643 -0.0004821 -0.03476 -0.7213 -2.1849
-1.6499 -0.7101 -0.1455 -0.02764 -0.004648 -0.0008124
-0.0002116; -0.00002949 -0.00008652 -0.006238 -0.1295 -0.3921
-0.2961 -0.1274 -0.02611 -0.004960 -0.0008341 -0.0001458
-0.00003798; 0 0 0 0 0 0 0 0 0 0 0 0; 0.00001609 0.00004642 0.003347
0.06947 0.2104 0.1589 0.06839 0.01401 0.002661 0.0004476 0.00007823
0.00002038; 0.00003770 0.0001106 0.007975 0.1655 0.5013 0.3786 0.1629
0.03338 0.006341 0.001066 0.0001864 0.00004856; 0.00008691 0.0002550
0.01839 0.3816 1.1558 0.8728 0.3757 0.07696 0.01462 0.002459
0.0004297 0.0001120; 0.0001805 0.0005295 0.03818 0.7923 2.4000 1.8123
0.7800 0.1598 0.03036 0.005105 0.0008923 0.0002325; 0.0003880 0.001138
0.08208 1.7033 5.1594 3.8962 1.6769 0.3435 0.06526 0.01098
0.001918 0.0004998; 0.0008309 0.002438 0.1758 3.6479 11.0496 8.3442
3.5914 0.7357 0.1398 0.02351 0.004108 0.001070; 0.001503 0.004410
0.318 6.5991 19.9887 15.0946 6.4968 1.3309 0.2528 0.04252
0.007432 0.001936];

figure
quiver(x,y,u,v,'b')
grid
```

A.6 MATLAB Codes for Fluid Mayonnaise of the Power-Law Model without the Integral Term

The M-file for fluid mayonnaise of the Power-Law model without the integral term to find x for $f(x) = 0$ by using the fzero function is named as

```
power_law_mayonnaise_fzero.m
```

and the codes are

```
function y=f(x)
y=-0.00981167*(x^0.55)+0.125;
```

The $u'(0) = -x$ found in the fzero function becomes an input in the ode15i() function. The M-file for the ode15i() function for the Power-Law model without integral term to plot the wave profile $u(x)$ is named as

```
power_law_model_code.m
```

and the codes are

```
f1=@(t,u,ud)[-0.00981167*(abs(ud)^(0.55))-0.5*(u^2)+0.5*u];
u0=[0.5]; ud0=[-102.186775]; u0F=[1]; ud0F=[];
[u0,ud0]=decic(f1,0,u0,u0F,ud0,ud0F);
r1=ode15i(f1,[0,0.15],u0,ud0);
r2=ode15i(f1,[0,-0.15],u0,ud0);
```

```
plot(r1.x,r1.y,'b',r2.x,r2.y,'b');
grid
```

The M-file for $u'(x)$ of the Power-Law model without the integral term is named as

```
power_law_ud.m
```

and the codes are

```
x=[-0.1000 -0.0939 -0.0839 -0.739 -0.0660 -0.0580 -0.0501 -0.0413
-0.0368 -0.0324 -0.0280 -0.0258 -0.0236 -0.0214 -0.0192 -0.0167 -0.0152
-0.0137 -0.0121 -0.0106 -0.0091 -0.0082 -0.0074 -0.0065 -0.0057 -0.0048
-0.0038 -0.0033 -0.0028 -0.0024 -0.0019 -0.0016 -0.0014 -0.0011 -0.0009
-0.0006 -0.0004 -0.0001 0 0.0001 0.0004 0.0006 0.0008 0.0010 0.0012
0.0014 0.0015 0.0017 0.0018 0.0019 0.0021 0.0022 0.0023 0.0024 0.0025
0.0026 0.0027 0.0028 0.0030 0.0032 0.0037 0.0041 0.0045 0.0049 0.0053
0.0057 0.0061 0.0065 0.0069 0.0074 0.0078 0.0084 0.0090 0.0096 0.0102
0.0107 0.0113 0.0119 0.0129 0.0139 0.0148 0.0157 0.0167 0.0176 0.0186
0.0196 0.0206 0.0215 0.0225 0.0235 0.0254 0.0274 0.0294 0.0313 0.0333
0.0352 0.0372 0.0391 0.0411 0.0431 0.0450 0.0470 0.0505 0.0540 0.0575
0.0611 0.0646 0.0681 0.0716 0.0751 0.0787 0.0822 0.0892 0.0955 0.1000];
ud=[-0.0368 -0.0432 -0.0551 -0.0738 -0.0980 -0.1325 -0.1885 -0.3147
-0.4182 -0.5827 -0.8434 -1.0337 -1.2893 -1.6225 -2.1075 -2.9024 -3.5985
-4.5502 -5.9133 -7.9117 -10.9473 -13.3362 -16.4646 -20.6028 -26.1590
-33.7313 -45.8887 -53.4753 -62.0281 -71.2970 -80.7630 -85.3129
-89.5900 -93.4356 -96.7319 -99.3298 -101.1330 -102.0688 -102.1868
-102.0688 -101.1330 -99.3298 -97.0158 -94.4692 -91.8398 -89.2549
-86.7795 -84.2240 -81.8234 -79.3949 -77.1560 -74.9390 -72.9156
-70.9212 -68.9367 -66.9400 -64.9639 -63.0137 -59.2103 -55.5643
-48.7601 -42.6990 -37.3803 -33.2185 -29.5611 -26.3931 -23.5854
-20.7966 -18.4214 -16.3866 -14.6236 -12.6826 -11.0618 -9.7360 -8.5958
-7.6276 -6.7985 -6.1978 -5.0582 -4.3203 -3.7356 -3.2574 -2.8471 -2.5116
-2.2218 -1.9754 -1.7670 -1.5791 -1.4311 -1.2893 -1.0700 -0.9021 -0.7704
-0.6625 -0.5757 -0.5008 -0.4429 -0.3941 -0.3478 -0.3147 -0.2831 -0.2579
-0.2197 -0.1842 -0.1594 -0.1400 -0.1253 -0.1079 -0.0980 -0.0886 -0.0795
-0.0709 -0.0602 -0.0502 -0.0455];

figure
plot(x,ud,'b')
grid
```

The M-file for the velocity vectors of the Power-Law model without the integral term is named as

```
power_law_model_quiver.m
```

and the codes are

```
x=[-0.1000 -0.0214 -0.0048 0 0.0021 0.0049 0.0113 0.0235
0.0505 0.1000];
y=[-0.1000 -0.0214 -0.0048 0 0.0021 0.0049 0.0113 0.0235
0.0505 0.1000];
u=[0.9968 0.9737 0.8378 0.5000 0.3108 0.1605 0.0599 0.0231 0.0086
```

```
0.0036; 0.9968 0.9737 0.8378 0.5000 0.3108 0.1605 0.0599 0.0231 0.0086
0.0036; 0.9968 0.9737 0.8378 0.5000 0.3108 0.1605 0.0599 0.0231 0.0086
0.0036; 0.9968 0.9737 0.8378 0.5000 0.3108 0.1605 0.0599 0.0231 0.0086
0.0036; 0.9968 0.9737 0.8378 0.5000 0.3108 0.1605 0.0599 0.0231 0.0086
0.0036; 0.9968 0.9737 0.8378 0.5000 0.3108 0.1605 0.0599 0.0231 0.0086
0.0036; 0.9968 0.9737 0.8378 0.5000 0.3108 0.1605 0.0599 0.0231 0.0086
0.0036; 0.9968 0.9737 0.8378 0.5000 0.3108 0.1605 0.0599 0.0231 0.0086
0.0036; 0.9968 0.9737 0.8378 0.5000 0.3108 0.1605 0.0599 0.0231 0.0086
0.0036; 0.9968 0.9737 0.8378 0.5000 0.3108 0.1605 0.0599 0.0231 0.0086
0.0036];
v=[-0.00368 -0.1623 -3.3731 -10.2187 -7.7156 -3.3214 -0.6799 -0.1289
-0.02197 -0.00455; -0.0007875 -0.03472 -0.7218 -2.1868 -1.6511 -0.7108
-0.1455 -0.02759 -0.004702 -0.0009737; -0.0001766 -0.007788 -0.1619
-0.4905 -0.3703 -0.1594 -0.03263 -0.006189 -0.001055 -0.0002184; 0 0 0
0 0 0 0 0 0 0; 0.00007728 0.003407 0.07084 0.2146 0.1620 0.06975
0.01428 0.002708 0.0004614 0.00009555; 0.0001803 0.007950 0.1653
0.5007 0.3781 0.1627 0.03331 0.006318 0.001077 0.0002230; 0.0004158
0.01833 0.3912 1.1547 0.8719 0.3753 0.07682 0.01457 0.002483
0.0005142; 0.0008648 0.03813 0.7927 2.4014 1.8132 0.7805 0.1598
0.03030 0.005163 0.001069; 0.001858 0.08194 1.7034 5.1604 3.8964
1.6773 0.3433 0.06511 0.01109 0.002298; 0.00368 0.1623 3.3731
10.2187 7.7156 3.3214 0.6799 0.1289 0.02197 0.00455];

figure
quiver(x,y,u,v,'b')
grid
```

Appendix B

MATLAB Information

The details about the MATLAB platform that we use for computations are
R2015a (8.5.0.197613)
64-bit (Win64)
License Number: 168486
The University of New Orleans
New Orleans, LA 70148
The United States of America

Bibliography

[1] A. Chertock, A. Kurganov, and Philip Rosenau. On degenerate saturated-diffusion equations with convection, Nonlinearity 18 (2005), pp. 609-630.

[2] A. H. K. Garakani, N. Mostoufi, F. Sadeghi, M. Hosseinzadeh, H. Fatourechi, M. H. Sarrafzadeh, M. R. Mehrnia. Comparison Between Different Models for Rheological Characterization of Activated Sludge. *Iran. J. Environ. Health. Sci. Eng., 2011, Vol. 8, No. 3, pp. 255-264*

[3] A. Kurganov,and P. Rosenau, Effects of a saturating dissipation in Burgers-type equations. *Communications on Pure and Applied Mathematics, Vol. L, 0753-0771 (1997)*

[4] B. R. Munson, A. P. Rothmayer, T. H. Okiishi, W. W. Huebsch . *Fundamentals of Fluid Mechanics*. Wiley. 7 edition (2012)

[5] D. Wei, and H. Borden. Traveling wave solutions of Burgers' equation for Power-law Non-Newtonian Flows. *Appl. Math. E-Notes, 11, electronic only (2011)*. pp. 133-138

[6] D. Wei and K. Holladay, "Travelling Wave Solutions of Burgers' Equation for Gee-Lyon Fluid Flows" *Applied Mathematics E-Notes, 12(2012), 129-135.*

[7] D. Xue, and Y. Chen, *Solving Applied Mathematical Problems with MATLAB*. CRC Press (2009)

[8] E. Hopf, The Partial Differential Equation $u_t + uu_x = \nu u_{xx}$. *Comm. Pure and Appl. Math., Vol.3 (1950)*. pp. 201-230.

[9] E. W.Weisstein. "Burgers' Equation." From MathWorld–A Wolfram Web Resource. http://mathworld.wolfram.com/BurgersEquation.html

[10] F. J. Murray, K. S. Miller.*Existence Theorems for Ordinary Differential Equations*. Washington Square, New York, New York Univ. Press, 1954.

[11] F. White. *Fluid Mechanics*. Seventh edition. McGraw-Hill Education, 2010.

[12] G. B. Whitham, Linear and nonlinear waves. *Pure and Applied Mathematics (New York).* John Wiley and Sons Inc., New York (1999). Reprint of the 1974 original, A Wiley-Interscience Publication.

[13] G. Astarita, and G. Marrucci, *Principles of Non-Newtonian Fluid Mechanics.* McGraw-Hill Book Company (UK) Limited, London, England, 1974.

[14] J. D. Cole, On a quasilinear parabolic equation occuring in aerodynamics. *Quart. Appl. Math.* Vol.9, No.3 (1951), pp. 225-236.

[15] J. D. Logan, An introduction to nonlinear partial differential equations. *Pure and Applied Mathematics (New York).* Wiley, John and Sons, Incorporated . A Wiley-Interscience Publication (1994)

[16] J. F. Steffe, *Rheological Methods in Food Process Engineering.* Second edition (second printing). Freeman Press, East Lansing, MI, USA, 1996.

[17] J. Goodman, A. Kurganov, and P. Rosenau, Breakdown in Burgers-type equations with saturating dissipation fluxes. IOP Publishing Ltd. and LMD Publishing Ltd., 1999.

[18] J. M. Burgers, A mathematical model illustrating the theory of turbulence. *Advances in Applied Mathematics.* Academic Press, 1948.

[19] L. Debnath, *Nonlinear Partial Differential Equations for Scientists and Engineers, Second edition.* Springer, 2005.

[20] M. Guedda, and Z. Hammouch, Similarity Flow Solutions of a Non-Newtonian Power-law Fluid. *International Journal of Nonlinear Science, Vol. 6 (2008), No. 3.* pp. 255-264.

[21] M. J. Lighthill and G. B. Whitham. On Kinematic Waves. II. A Theory of Traffic Flow on Long Crowded Roads. Proc. R. Soc. Lond. A 10 May 1955 vol. 229 no. 1178 317-345

[22] M. M. Cross, Rheology of non-Newtonian fluids - a new flow equation for pseudoplastic systems. *J. Colloid Sci., 20(5): 417-437 (1965).*

[23] M. U. Tyn, and L. Debnath, *Partial Differential Equations for Scientists and Engineers, 3^{rd} Edition.* PTR Prentice-Hall, Upper Saddle River, New Jersey, 1987.

[24] M. V. Ochoa, *Analysis of Drilling Fluid Rheology and Tool Joint Effect to Reduce Errors in Hydraulics Calculations*, Ph.D. dissertation, Texas A and M Univ., 2006.

[25] P. I. Richards, *Shock Waves on the Highway. Operations Research, 4 (1956).* pp. 42-51

[26] P. K. Kythe,and D. Wei, *An Introduction to Linear and Nonlinear finite Element Analysis: A Computational Approach*. Birkhauser, 2004.

[27] R. B. Bird, C. F. Curtiss, R.C.Armstrong, and O. Hassager, *Dynamics of Polymeric Liquids, Vol. 1-2*. Wiley-Interscience, New York, 1987.

[28] R. E. Gee and J. B. Lyon, Nonisothermal flow of viscous non-Newtonian fluids. *Ind. Eng. Chem., 49 (6)*, 1957.

[29] S. S. Shibeshi,W. E. Collins. the Rheology of blood flow in a branched arterial system. *Appl. Rheol., 15(6)*, (2005)398-405.

[30] S. C. Chapra, *Applied Numerical Methods with MATLAB for Engineers and Scientists*. Third edition. McGraw-Hill Education, 2011.

[31] U. R. Charrondiere, D. Haytowitz, and B. Stadlmayr.FAO/INFOODS (2012). FAO/INFOODS Density Database Version 2.0. FAO, Rome.

[32] V. Camacho, R. D. Guy and J. Jacobsen, Traveling waves and shocks in a viscoelastic generalization of Burgers' equation. *SIAM J. APPL. MATH. Vol. 68 (2008).No.5*. pp. 1316-1332.

[33] W. Alpha, Wolfram Alpha LLC. http://www.wolframalpha.com/input/?i=power+series+expansion+integral+of+0.270059%2F%281%2B0.401552*%28y^0.969%29%29+dy+at+y%3D1 (2015)

[34] W. Alpha, Wolfram Alpha LLC. http://www.wolframalpha.com/input/?i=power+series+expansion+integral+of+0.0753686*%281%2B1.327104*%28y^2%29%29^%280.305%29+dy+at+y%3D1 (2015)

[35] W. L. Wilkinson, *Non-Newtonian Fluids:Fluid Mechanics, Mixing and Heat Transfer*. Pergamon Press, New York, 1960.

[36] Y. G. Rykov, On the theory of discontinuous solutions to some strongly degenerate parabolic equations, arXiv:math/0105174v1 [math.AP] (2001)

[37] Y. C. Fung,*Biomechanics.Mechanical Properties of Living Tissues*. Springer, 1993.

Vita

The author, *Yupeng Shu*, registered as a graduate student in the Department of Mathematics, the University of New Orleans in August 2013 to pursue his Ph.D. in Engineering and Applied Science. Before that, he graduated from the University of New Orleans with Bachelor of Science degrees in two mutually independent majors, i.e., Mathematics and Physics, in May 2013. This manuscript serves as his thesis for the Master of Science in Mathematics.

His current research interests include applied mathematics, applied physics, fluid mechanics, and signal and image processing.